J. Iran. Chem. Soc., Vol. 7, No. 1, March 2010, pp. 1-37.

JOURNAL OF THE
Iranian
Chemical Society

Magnetic Nanoparticles: Synthesis, Stabilization, Functionalization, Characterization, and Applications

M. Faraji, Y. Yamini* and M. Rezaee
Department of Chemistry, Tarbiat Modares University, P. O. Box 14115-175, Tehran, Iran

(Received 20 October 2009, Accepted 10 January 2010)

This review focuses on the synthesis, protection, functionalization, characterization and with some applications of magnetic nanoparticles (MNPs). The review begins with an overview on magnetic property and single domain particles. The synthetic strategies developed for the generation of MNPs, with a focus on particle formation mechanism and recent modifications made on the synthesis of monodisperse samples of relatively large quantities are also discussed. Then, different methodologies for the protection and functionalization of the synthesized MNPs, together with the characterization techniques are explained. Finally, some of the recent industrial, biological, environmental and analyticals application of MNPs are briefly reviewed, and some future trends and perspectives in these research areas will be outlined.

Keywords: Magnetic nanoparticles, Synthetic methods, Protection and functionalization techniques, Characterization, Applications

INTRODUCTION

Nanoscience is one of the most important research and development frontiers in modern science. The use of nanoparticles (NPs) materials offers many advantages due to their unique size and physical properties. Because of the widespread applications of magnetic nanoparticles (MNPs), in biomedical, biotechnology, engineering, material science and environmental areas [1-8], much attention has been paid to the preparation of different kinds of MNPs. The synthesis of uniform-sized (or monodisperse, with a relative standard deviation of < 5%) nanocrystals is of key importance because the properties of these nanocrystals depend strongly on their dimensions [9-15]. From the fundamental scientific viewpoint, the synthesis of uniform-sized nanocrystals with controllable sizes is very important to characterize the size-dependent physical properties of nanocrystals [13-15]. To date, a number of preparation methods for MNPs have been developed, such as chemical coprecipitation, microemulsion and thermal decomposition. Although monodispersed MNPs have been synthesized using some of these methods, precise control of their size, shape and surface is generally challenging. On the other hand, the production of large quantities of uniform-sized nanocrystals will become critical for the realization of high-quality nanoscale devices and many nanotechnological applications. For example, the color sharpness of semiconductor nanocrystalbased optical devices and biomedical imaging probes is strongly dependent on the uniformity of the nanocrystals [16-20], and also all biomedical application requires that the nanoparticles have high magnetization values, with sizes smaller than 100 nm, and a narrow particle size distribution. Over the past decade, remarkable advances and modifications have been made in the synthesis of uniform-sized colloidal nanocrystals [21-28]. Therefore, to get more information about MNPs and to improve their applications or develop new ones, are essential

*Corresponding author. E-mail: yyamini@modares.ac.ir

careful studies related to their stability, functionality, particle sizes and also their materials and physical behaviours. It is noteworthy that in many cases the protecting outer shells not only stabilize the nanoparticles, but they can also be used for further functionalization, for instance, with other nanoparticles or various ligands, depending on the desired application. Functionalized nanoparticles are very promising in their applications as catalysis, or in biolabeling and bioseparation.

In this review, the synthesis methods of MNPs, fluid stabilization (using electrostatic layer or sterical repulsion), surface functionalization depend on application, the different techniques for structural and physicochemical characterization will be summarized then some industrial, biomedical, environmental and analytical applications will be presented.

MAGNETIC PROPERTY

Magntic Behavior

Materials are classified by their response to an externally applied magnetic field. Descriptions of orientations of the magnetic moments in a material help to identify different forms of magnetism observed in nature. Five basic types of magnetism can be described: diamagnetism, paramagnetism, ferromagnetism, antiferromagnetism and ferrimagnetism. In the presence of an externally applied magnetic field the atomic current loops created by the orbital motion of electrons respond to oppose the applied field. All materials display this type of weak repulsion to a magnetic field known as diamagnetism. However, diamagnetism is very weak and therefore any other form of magnetic behavior that a material may possess usually overpowers the effects of the current loops. In terms of the electronic configuration of materials, diamagnetism is observed in materials with filled electronic subshells where the magnetic moments are paired and overall cancel each other. Diamagnetic materials have a negative susceptibility ($\chi < 0$) and weakly repel an applied magnetic field (*e.g.*, quartz SiO_2). The effects of these atomic current loops are overcome if the material displays a net magnetic moment or has a long-range ordering of its magnetic moments [29]. All other types of magnetic behaviors are observed in materials that are at least partially attributed to unpaired electrons in their atomic shells, often in the 3d or 4f shells of each atom. Materials whose atomic magnetic moments are uncoupled display paramagnetism, thus paramagnetic materials have moments with no long-range order and there is a small positive magnetic susceptibility ($\chi \approx 0$); *e.g.*, pyrite [29]. Materials that possess ferromagnetism have aligned atomic magnetic moments of equal magnitude and their crystalline structures allows for direct coupling interactions between the moments, which may strongly enhance the flux density (*e.g.*, Fe, Ni and Co). Furthermore, the aligned moments in ferromagnetic materials can confer a spontaneous magnetization in the absence of an applied magnetic field. Materials that retain permanent magnetization in the absence of an applied field are known as hard magnets. Materials having atomic magnetic moments of equal magnitude that are arranged in an antiparallel fashion display antiferromagnetism (*e.g.*, troilite FeS). The exchange interaction couples the moments in such a way that they are antiparallel therefore leaving a zero net magnetization [30]. Above the Neel temperature (T_N) thermal energy is sufficient to cause the equal and oppositely aligned atomic moments to randomly fluctuate leading to a disappearance of their long range order. In this state the materials exhibits paramagnetic behavior. Ferrimagnetism is a property exhibited by materials whose atoms or ions tend to assume an ordered but non-parallel arrangement in zero applied field below a certain characteristic temperature known as the Neel temperature (*e.g.*, Fe_3O_4 and Fe_3S_4). In the usual case, within a magnetic domain, a substantial net magnetization results from the antiparallel alignment of neighboring non-equivalent sublattices. The macroscopic behavior is similar to ferromagnetism. Above the Neel temperature, the substance becomes paramagnetic.

Superparamagnetism Phenomenon

Domains, which are groups of spins all pointing in the same direction and acting cooperatively are separated by domain walls, which have a characteristic width and energy associated with their formation and existence. The motion of domain walls is a primary means of reversing magnetization. Experimental investigation of the dependence of coercivity on particle size showed a behavior similar to that schematically illustrated in Fig. 1 [23]. Size reduction in magnetic materials (multi-domain materials) resulting in the formation of single-domain particles also gives rise to the phenomenon of superparamagnetism. Briefly, superparamagnetism occurs

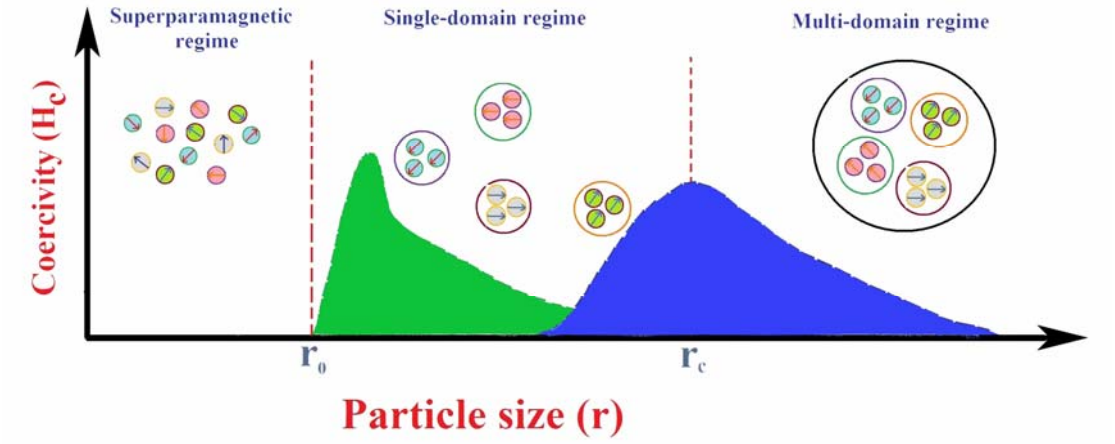

Fig. 1. Schematic illustration of the dependence of coercivity on particle size [23].

when thermal fluctuations or an applied field can easily move the magnetic moments of the nanoparticle away from the easy axis, the preferred crystallographic axes for the magnetic moment to point along. Each particle behaves like a paramagnetic atom, but with a giant magnetic moment, as there is still a well-defined magnetic order in each nanoparticle [25,31]. Superparamagnetic materials are intrinsically nonmagnetic but can be readily magnetized in the presence of an external magnetic field. The critical radius r_C for different particles differ based on shape, temperature and crystalline magnetoanisotropy [23,24].

SYNTHETIC METHODS

During the past decade, great efforts have been devoted to the preparation of MNPs due to their potential applications in many diverse fields. MNPs have been synthesized with a number of different compositions and phases, including pure metals Fe, Co and Ni [33-35]; metal oxides, such as Fe_3O_4 and γ-Fe_2O_3 [36-38]; ferrites, such as MFe_2O_4 (M = Cu, Ni, Mn, Mg, *etc.*) [39,40]; and metal alloys, such as FePt, CoPt [41,42]. During the last few years, a large portion of the published articles about MNPs have described efficient routes to attain shape-controlled, highly stable, and narrow size distribution MNPs. Up to date, several popular methods including co-precipitation, microemulsion, thermal decomposition, solvothermal, sonochemical, microwave-assisted, chemical vapour deposition, combustion synthesis, carbon arc, laser pyrolysis synthesis have been reported for synthesis of MNPs.

LIQUID PHASE SYNTHSIS

The principles by which monodisperse (with a relative standard deviation of ~ 5%) particles can be prepared are readily presented in a diagram due to LaMer (Fig. 2). As described in the LaMer diagram [12], for homogeneous precipitation, as concentration increases to pass its saturation, it reaches a point where nucleation occurs. Particle growth most likely transpires by a combination of the diffusion of atoms onto the nuclei and with irreversible aggregation of nuclei. The requirements for monodispersity are evident from the LaMer diagram:

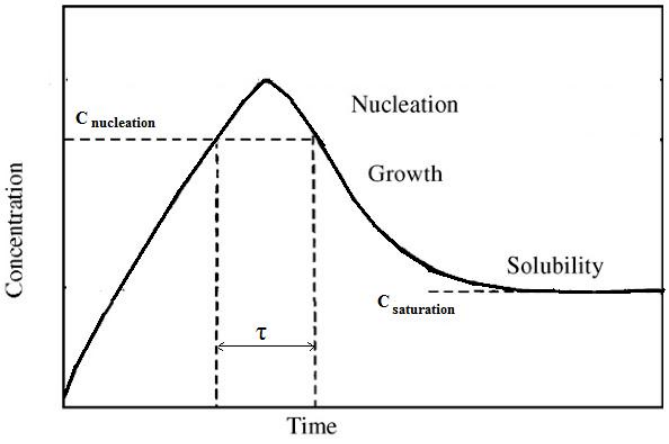

Fig. 2. LaMer diagram.

(I) The rate of nucleation must be high enough so that the concentration does not continue to climb. Instead, a burst of nuclei are created in a short period (τ short).
(II) The rate of growth of these nucleis must be fast enough to reduce the concentration below the nucleation concentration point, quickly. In this way only a limited number of particles are created.
(III) The rate of growth must be slow enough, however, that the growth period is long compared with the nucleation period. This usually narrows the size of distribution which results from finite nucleation period.

So, by controlling these factors monodisperse MNPs with different sizes can be synthesized.

Co-precipitation

Co-precipitation is a facile and convenient way to synthesize MNPs (metal oxides and ferrites) from aqueous salt solutions. This is done by the addition of a base under inert atmosphere at room temperatures or at elevated temperature. Iron oxide nanoparticles (either Fe_3O_4 or γ-Fe_2O_3) and ferrites are usually prepared in an aqueous medium which chemical reaction of formation may be written as Eq. (1).

$$M^{2+} + 2Fe^{3+} + 8OH^{-} \rightarrow MFe_2O_4 + 4H_2O \quad (1)$$

Where M can be Fe^{2+}, Mn^{2+}, Co^{2+}, Cu^{2+}, Mg^{2+}, Zn^{2+} and Ni^{2+}. Complete precipitation should be expected at a pH levels between 8 and 14, with a stoichiometric ratio of 2:1 (Fe^{3+}/M^{2+}) in a non-oxidizing oxygen environment [44]. Magnetite nanoparticles (Fe_3O_4) are not very stable under ambient conditions, and are easily oxidized to be a maghemite or dissolved in an acidic medium. Since maghemite (γ-Fe_2O_3) is ferrimagnet, making its oxidation is the lesser problem. Therefore, magnetite particles can be subjected to deliberate oxidation to convert them into a maghemite [24]. The size, shape, and composition of the MNPs very much depends on the type of salts used (*e.g.* chlorides, sulfates, nitrates), the M^{2+}/Fe^{3+} ratio, the reaction temperature, the pH value, plus type of base, also the mixing rate, ionic strength of the media, with the addition sequence and bubbling of nitrogen gas are all important.

Iida *et al.* [8] synthesized Fe_3O_4 nanoparticles by hydrolysis in an aqueous solution containing ferrous and ferric salts at various ratios with a 1,6-hexanediamine as the base. They found that when the ratio of ferrous to ferric ions was increased, the formation of large hydroxide particles as a precursor of Fe_3O_4 was promoted, which resulted in an increase in the size of Fe_3O_4 nanoparticles. As a result, the mean diameter of Fe_3O_4 nanoparticles increased from ~9 to ~37 nm as the molar percentage of ferrous ions with respect to the total iron ions was increased from 33 to 100%. Also, it was demonstrated that magnetic properties of Fe_3O_4 nanoparticles can be controlled by adjusting the molar ratio of ferrous to ferric ions as well as the particle diameter. Furthermore, the saturation magnetization values of the samples synthesized with both ferrous and ferric salts were 46.7 and 55.4 emu g^{-1} for sulfate and chloride, respectively. These results are corroborated by literature data [45,46].

Another most important factor influencing the synthesis is the iron concentration which generally the optimum values are between 39 and 78 mM [26]. In the synthesis of Fe_3O_4, precipitation at temperatures below 60 °C typically produces an amorphous hydrated oxyhydroxide that can be easily converted to Fe_2O_3, while higher reaction temperatures (>80 °C) favor the formation of Fe_3O_4 [47,48]. The suitable pH for the rapid formation of Fe_3O_4 is attained by the addition of excess amounts of the base. Shen *et al.* observed that the product showed a brownish color, an indication of the presence of Fe_2O_3, if the precipitation temperature was below 60 °C or insufficient NH_4OH was added [49]. Hong *et al.* [50] observed that when Fe_3O_4 nanoparticles precipitated using NH_4OH instead of NaOH a better crystallinity, higher saturation magnetization and smaller size can be observed [51].

Qiu *et al.* [52] investigated the dependence of the ionic strength on the reaction solution in the formation of magnetite NPs. The magnetite prepared with the addition of 1 M NaCl in an aqueous solution is smaller than those formed without its addition. However, these smaller nanoparticles formed in higher ionic strength solutions display a lower saturation magnetization (63 emu g^{-1}) than those prepared in NaCl-free solutions (71 emu g^{-1}). The lower magnetization is attributed to the decrease in size of the particles when prepared in higher ionic strength medias.

An increase of the mixing rate tends to decrease the particle size. In the same way, a decrease of size as well as the

polydispersity is observed when the base is added to the reactive in comparison with opposite process [53].

Nitrogen gases' bubbling through the solution not only protects against critical oxidation of the magnetite NPs but also reduces the particle size when compared to methods without oxygen removal [54,55]. Recently, Hong *et al*. [50] used $N_2H_4.H_2O$ as an oxidation-resistant reagent. Based on their study, hydrazine can react with the dissolved oxygen to form $[NH_3OH]^+$ as in the following equation:

$$N_2H_4.2H_2O + 4H^+ + 0.5O_2 \leftrightarrow 2[NH_3OH]^+ \quad (2)$$

The cationic $[NH_3OH]^+$ can also react with Fe^{2+} to form Fe_3O_4 as follows:

$$3Fe^{2+} + [NH_3OH]^+ + 6OH^- \rightarrow Fe_3O_4 + [NH_4]^+ + 3H_2O \quad (3)$$

Liu *et al*. [56] declared that when the diluted water is not deoxygenated and the synthesis proceeds under air without the protection of N_2 gas, the prepared colloids are reddish-brown which indicates that there is a contamination of other iron oxides phases in the colloids as a result of the strong oxidation. Fe_3O_4 might be oxidized as:

$$Fe_3O_4 + 0.25O_2 + 4.5H_2O \rightarrow 3Fe(OH)_3 \quad (4)$$

This would critically affect the magnetic properties of nanosized particles and the M_s is decreased 35% comparing to former reactions. So it is necessary to introduce N_2 gas in the synthesis to avoid the unwanted oxidation. Also, if the alkali sources are poured as quickly as possible into the ironic solution under vigorous stirring conditions, black colloid can be obtained but the size distribution is wide and some precipitation is found after several weeks. This indicates that the rate of nucleation and crystalline growth are high indicating that the sizes of the particles are not properly controlled [56].

In terms of simplicity of the synthesis method, co-precipitation is the preferred route. In this method, the reaction temperature and time are lower than other methods such as thermal decomposition and hydrothermal. Also, solvent is environmental friendly (water) besides the reaction yield is high and scalable. But, size distribution is relatively narrow and the shape control is not good.

Microemulsion

The water-in-oil (W/O) microemulsion, has been widely used to synthesize uniform sized MNPs [57-62]. This is an isotropic and thermodynamically stable single-phase system that consists of three components: water, oil and an amphiphilic molecule, called surfactant. The surfactant molecule lowers the interfacial tension between water and oil resulting in the formation of a transparent solution. The water nanodroplets containing reagents, as a nanoreactor, undergo rapid coalescence allowing for a mixing, precipitation reaction and an aggregation processes for the synthesis of MNPs. The shape of the water pool is spherical and the surfactant molecules surround the nanodroplet wall. These walls act as cages for the growing particles and thereby reduce the average size of the particles during the collision and aggregation process. Thus, the size of the spherical nanoparticles can be controlled and tuned by changing the size of the water pool (W_0 value, the water-to-surfactant molar ratio). Generally, the higher values of W_0, give the larger particle size. By mixing two identical water-in-oil microemulsions containing the desired reactants, the microdroplets will continuously collide, coalesce and break again, and finally a precipitate forms in the micelles.

Santra *et al.* [62] reported a robust methodology for the synthesis of both uncoated and silica-coated MNPs of ultrasmall (<5 nm) and a very uniform size distribution by water-in-oil microemulsion. They used three different nonionic surfactants (Triton X-100, Igepal CO-520 and Brij-97) for the preparation of microemulsions, and also used NH_4OH and NaOH as base source. By mixing two identical water-in-oil microemulsions which one of them containing metal salts and the other containing the base source, microdroplets will continuously collide, coalesce, and break again and finally a precipitate forms in the micelles. By addition of solvents, such as acetone or ethanol, to the microemulsions, the precipitate can be extracted by filtering or centrifuging the mixture. They found that depending on the chemical structure of the surfactant molecules the extent of surfactant molecule adsorption onto the surface of the NPs varies. A more ordered fashion in particle aggregation is observed in the case of Brij 97 when compared to the other

surfactants, because of a strong hydrophobic-hydrophobic interaction between oleyl groups attached to adjacent nanoparticles. On the hand, Vidal-Vidal *et al*. [63] reported the synthesis of monodisperse magnetite NPs with the use of one point microemulsion method. The spherical shaped particles, capped with a monolayer coating of oleylamine (or oleic acid), show a narrow size distribution of 3.5 ± 0.6 nm, are well crystallized and have high saturation magnetization values. Moreover, the results show that oleylamine acts as a precipitating and capping agent. However, cyclohexylamine acts only as a precipitating agent and does not avoid particle aggregation. Microemulsions can be used to synthesize monodispersed nanoparticles with various morphologies. However, this method requires a large amount of solvent and also the yield of production of this method is low.

Thermal Decomposition

Nanoparticles with a high level of monodispersity and size control can be obtained by high-temperature decomposition of organometallic precursors, such as $[M^{n+}(acac)_n]$, (M = Fe, Mn, Co, Ni, Cr; n = 2 or 3, acac = acetylacetonate), $M^x(cup)_x$ (cup = N-nitrosophenylhydroxylamine) or carbolys (such as $Fe(CO)_5$) using organic solvents and surfactants such as fatty acids, oleic acid and hexadecylamine. Thermal decomposition of organometallic precursors which metal is the zerovalent in their composition (such as $Fe(CO)_5$) initially leads to a formation of metal NPs but if followed by oxidation can lead to a high in quality monodispersed metal oxides. On the other hand, decomposition of precursors with cationic metal centers (such as Fe $(acac)_3$) leads directly to metal oxides NPs.

Principally the ratios of the starting reagents including organometallic compounds, surfactants, and solvents are the decisive parameters for controlling the size and morphology of MNPs. The reaction temperature and time, as well as the aging period may also be crucial for the precise control of size and morphology [24]. The effect of reaction temperatures and reaction times on size, morphology and magnetic properties of nanoparticles are schematically shown in Fig. 3 [64].

Chen *et al*. [65] prepared nickel NPs from the thermal decomposition of nickel(II) acetylacetonate in alkylamines. The reaction temperature, heating rate and solvent type all played an important role in the control over the crystalline phase in their study. They found that by choosing an appropriate reaction temperature and solvent, nickel NPs that have the fcc or the hcp phase can be obtained. Monodisperse nickel NPs were also obtained by introducing surfactants. Also, the results of magnetic characterization showed that the magnetic properties of the hcp nickel NPs are quite different from those of the fcc nickel NPs.

Metal oxide MNPs can also be synthesized by the thermal decomposition method. Up to date, two different approaches have been used for this purpose. First, thermal decomposition of metal carbonyl precursors followed by an oxidation step using air [66], or oxidation by using an oxidant at elevated temperatures [67]. The second is decomposition of precursors with a cationic metal center in the absence of reducing agents [68]. The presences of reducing agents lead to metal NPs even by the use of cationic precursors [69].

Thermal decomposition seems the best method developed to date for size and morphology control of NPs. Also, the yield

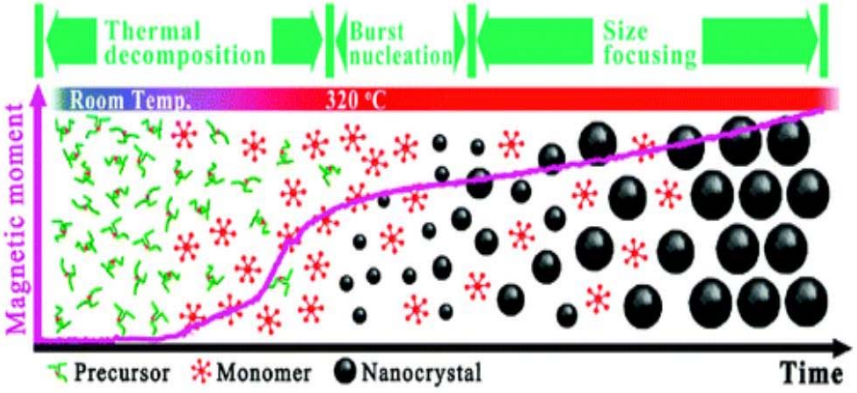

Fig. 3. Effect of reaction temperature and reaction time on size, morphology and magnetic properties of MNPs [64].

of production is high and scalable. However, one of the major disadvantages of this method is the production of organic-soluble NPs which limit the extent of application uses of them in biological fields besides surface treatment is needed after synthesis; also, thermal decomposition methods usually lead to complicated processes or require relatively high temperatures.

Solvothermal Routs

Hydrothermal, also called solvothermal, is a syntheses method for preparation of MNPs and ultrafine powders in literature [70-76]. These reactions are performed in an aqueous media in reactors or autoclaves where the pressure can be higher than 2000 psi and temperatures higher than 200 °C. Hydrothermal processing is one of the successful ways to grow crystals of many different materials. This technique has also been used to grow dislocation free single crystal particles, and grains formed in this process could have a better crystallinity than those from other processes.

Wang *et al*. [74] used a hydrothermal method to synthesize Fe_3O_4 powder. They found that the nanoscale Fe_3O_4 powder (40 nm) can be obtained at 140 °C for 6 h possessed a saturation magnetization of 85.8 emu g^{-1}, this is a little lower than that of the correspondent bulk Fe_3O_4 (92 emu g^{-1}). It is suggested that the well crystallized Fe_3O_4 grains formed under appropriate hydrothermal conditions should be responsible for the increased saturation magnetization in nanosized Fe_3O_4. The well-crystallized particles have a thinner surface layer, narrower cationic distribution and less superamagnetic relaxation, which can be used to explain the increase of saturation magnetization in hydrothermal derived particles, and to interpret magnetic property variation from different conditions in hydrothermal process, because they would lead to different crystallinity of particles.

Polyethyleneglycol (PEG)-assisted hydrothermal route is another mode of the hydrothermal technique which has been extensively used for the synthesis of MNPs [75,76]. Wang *et al*. successfully synthesized size-controlled nickel ferrite NPs *via* a simple solvothermal method by using ethylene glycol as solvent and NaAc by electrostatic stabilization. They easily controlled the size of the NPs from 6 to 170 nm by adjusting the experimental parameters such as the reaction duration, initial concentration of the reactants, amount of protective reagents and the type of acetates [76].

In recent years, automation of the hydrothermal method has been investigated by the Teja's research group [77-79]. Continuous hydrothermal processing (CHP) offers a relatively simple route to make metal oxide NPs of specific sizes and morphology [77]. The method is environmentally benign and amenable to scale-up, although the mechanisms of particle formation have yet to be determined. Xu *et al*. [79] investigated factors that affect the size, distribution size, and morphology of α-Fe_2O_3 nanoparticles obtained *via* continuous hydrothermal synthesis. In their study, in presence of polyvinyl alcohol (PVA) during synthesis aggregation of particles can be limited and size distributions is narrower than in the absence of PVA. Findings showed as well that the average particle size increases with temperature and residence time; besides it is accompanied by morphology changes in some cases.

Although hydrothermal technique is very versatile, one of the main drawbacks of the conventional hydrothermal method is the slow reaction kinetics at any given temperature. Microwave heating can be used during the hydrothermal synthesis and this has been found to increase the kinetics of crystallization [80]. Such a combination is termed the microwave-hydrothermal method. The main advantage of the introduction of microwaves into a reaction system is the extremely rapid kinetics needed for synthesis. A dramatic increase in the reaction kinetics, up to two orders of magnitude, can be achieved by the microwave heating under hydrothermal conditions, due to the localized super heating of the solution. Sreeja *et al*. [81] synthesized γ-Fe_2O_3 nanoparticles by the microwave-hydrothermal method. They declared that microwave-hydrothermal method is a convenient, fast and single step process for the synthesis of nanoparticles of γ-Fe_2O_3. NPs of γ-Fe_2O_3 could be synthesized at 150 °C in shorter time duration, (25 min) by this method with a much lower temperature and reaction time in comparison with conventional hydrothermal methods.

Chemical Reduction

Among the various solution-phase chemistry routes developed for the preparation of metal NPs, the reduction of metal salts is the most common, and reducing agents such as $NaBH_4$ [82-85] have been commonly employed in the reactions. Nanoscale zero-valent iron (nZVI) which have been

extensively used in the environmental remediation field, have commonly been prepared by mixing equal volumes of $NaBH_4$ and $FeCl_3$, the following reaction of:

$$4Fe^{3+} + 3NaBH_4 + 9H_2O \rightarrow 4Fe^0 \downarrow + 3NaH_2BO_3 + 12H^+ + 6H_2 \quad (5)$$

A key advantage of this method is its simplicity. It can be safely done in most chemistry labs with simple chemical reagents. Also, this reaction can be done at room temperature conditions.

Sonochemical Reactions

As a competitive alternative to other time-consuming preparation techniques, the sonochemical method has been extensively used to generate novel materials with unusual properties. The physiochemical effects of ultrasound arise from acoustic cavitation, which comes from the formation, growth and implosive collapsing of bubbles in the liquid. The implosive collapsing of the bubbles generate a localized hotspot through adiabatic compression or shock wave formation within the gas phase of the collapsing bubble. The conditions formed in these hotspots have been experimentally determined, with transient temperatures of 5000 K, pressures of 1800 atm and cooling rates beyond 10^{10} K s^{-1}. These extreme conditions were beneficial to forming the new phase and have a shear effect for agglomeration, which is necessary to prepare the high monodispersive nanoparticles [86]. Kim *et al*. [87] synthesized Fe_3O_4 NPs by the use of sonochemical and co-precipitation methods. The crystallinity and magnetic properties of the obtained products by the use of the two methods were compared and obtained results showed that those of Fe_3O_4 NPs from the sonochemical method had a higher crystallinity and saturation magnetization than those obtained from the co-precipitation method.

Microwave Method

The microwave-assisted solution method has become widely used due to its advantages such as its rapid volumetric heating, higher reaction rate, reducing reaction time and increasing yield of products compared to conventional heating methods [88,89]. Wang [90] reported synthesis of the spinel structured $M^{II}Fe_2O_4$ (M = Co, Mn) nanoparticles with diameters less than 10 nm by a fast and simple microwave-assisted polyol process. The small particle sizes are probably the results of the fast and homogeneous reactions occurring during the microwave synthesis. They found that the reaction temperature and crystal quality could be controlled by adjusting the volume ratio of distilled water to EG under microwave heating. Wang and co-workers also reported application of the simple microwave heating method for preparation of magnetite (Fe_3O_4) and hematite (α-Fe_2O_3) using $FeCl_3$, polyethylene glycol and $N_2H_4.H_2O$ [91]. They found that the amount of $N_2H_4.H_2O$ has an effect on the final phase of Fe_3O_4. At higher amounts of $N_2H_4.H_2O$ only the single phase of Fe_3O_4 can be formed but at lower amounts the product consisted of mixtures of Fe_3O_4 and α-Fe_2O_3. In addition, they reported that the heating method plays an important role in the shape of nanocrystals. Ellipsoidal α-Fe_2O_3 nanoparticles were prepared by microwave heating. While a mixture of irregular α-Fe_2O_3 NPs and rods were prepared by oil bath.

The main advantage of the introduction of microwaves into the reaction system is in obtaining an extremely rapid kinetic for crystallization, which may be attributed to the localized superheating of the solutions under microwave heating. While, in other techniques such as co-precipitation, thermal decomposition, *ect*., procedures for the improvement of the crystallinity is needed to high reaction times which this is the reason for the high energy consummation.

GAS PHASE SYNTHSIS

Chemical Vapour Deposition

Gas phase methods for preparing nanomaterials depend on thermal decomposition (pyrolysis), reduction, hydrolysis, disproportionation, oxidation, or other reactions to cause precipitation of solid products from the gas phase [92]. In the chemical vapor deposition (CVD) process, a carrier gas stream with precursors are delivered continuously by a gas delivery system to a reaction chamber maintained under a vacuum at high temperature (>900 °C) [93,94]. The CVD reactions take place in the heated reaction chamber and the products combine to form clusters of NPs. Growth and agglomeration of the particles are mitigated *via* the rapid expansion of the two-phase gas stream at the outlet of the reaction chamber.

The subsequent heat treatment of the synthesized

nanopowders in the various high-purity gas streams allows compositional and structural modifications, including particle purification and crystallization, as well as transformation into a desirable size, composition, and morphology [92,93]. The CVD process has been employed to deposit iron oxide by the reaction of a halide, such as iron trichloride, with water at 800-1000 °C [95]. The success of this method depends on the low concentrations of the precursor in the carrier gas, as well as rapid expansion and then the quenching of the nucleated clusters or nanoparticles as they exit from the reactor [92,93].

Recently, catalytically assisted chemical vapour deposition (CCVD) has become increasingly important because of its potential for scalable production [96]. However, this potential cannot be practically realized until some obstacles have been overcome [97,98], such as the relatively low productivity, the existence of complex phases, and the difficulty in separating carbon-encapsulated superparamagnetic NPs (CESNs) from the impurities.

Arc Discharge

Most carbon-encapsulated MNPs (CEMNPs) have been synthesized by using the arc discharge method in which metal precursors are usually packed inside a cave drilled into a graphite electrode and then subjected to arc vaporization [99-101]. Magnetic metal carbides can be encapsulated in the carbon using this method. The arc discharge method has also been proposed to coat metal NPs with boron nitride (BN) [102-104].

Dravid and co-workers [99,100] modified the arc discharge method and successfully produced nanophase Ni encapsulated in graphitic shells. In this case, the product usually consisted of mixtures of different forms of carbon, including carbon nanotubes, carbonencapsulated metal particles and graphitic flakes. In addition, the metal particles had a wide size distribution.

Sun *et al*. [105] also developed a modified arc discharge (carbon arc) method for synthesising of carbon encapsulated NPs of Fe, Ni and Co, with average sizes lower than 15 nm. For three carbon encapsulated materials, nanoparticles in both the metallic phase (α-Fe, γ-Fe; hcp-Co, fcc-Co; fcc-Ni) and also in the carbide phase (M_3C, M = Fe, Co, Ni) were characterized by being encapsulated in graphitic carbon. Borysiuk *et al*. [106] discussed about the formation of NPs in an arc discharge. The authors declared that plasma-arc samples were synthesized *via* using dual mechanisms: growth of nanocrystals from the vapor phase (carbide) and solidification of the liquid micro-droplets in the cold zone (α-Fe and γ-Fe).

Despite intensive research on optimizing the methods for depositing carbon encapsulated ferromagnetic NPs; the effect of the carbon cages remains unclear.

Recently, Ang *et al*. [107] synthesized carbon encapsulated Ni particles using an electric arc discharge in de-ionized water between a solid graphite cathode and an anode consisting of Ni and C in the mass ratio of Ni:C = 7:3. The natural separation of the produced material at different depths of the water container has enabled for the examination of size-dependent magnetic properties. They found that the diamagnetic contribution of the carbon capsules reduces the magnetic moment of the core, an effect that becomes more prominent as the particle sizes decrease.

Unfortunately the arc discharge method is not suitable for the coating of the large quantities of NPs needed for in the industrial production due to its low production yields. In addition, there is the difficulty in the control of particle sizes as well as the nanocoating's thickness. The product usually consisted of mixtures of different forms of carbon and separating of CEMNPs from impurities is difficult both of which makes the method cumbersome.

Laser Pyrolysis

Laser light heats a gaseous mixture of iron precursor and a flowing mixture of gases and produce small, narrow sized, non aggregated NPs. When the experimental conditions of pyrolysis are adjusted, the crystal sizes of magnetite NPs are varied, in the range from 2 to 7 nm with a very narrow size of distribution. Laser pyrolysis as a technique for the preparation of iron-based nanostructures, it is used where sensitized iron-pentacarbonyl-based mixtures and ethylene, as an energy-transfer agent are employed using air, as an oxidant [108-111].

Laser pulse has been applied in the synthesis of MNPs in the liquid phase, too [112,113]. Ye *et al*. [112] reported a new method to synthesize graphite-coated iron NPs by pulsed laser decomposition of a deoxygenated hexane solution in which $Fe_3(CO)_{12}$ and PPh_3 are dissolved. In their study, the authors explained that PPh_3 is the essential ingredient in the solution, which produces graphite-coated iron NPs. Park *et al*. [113]

developed a method to synthesize CEMNPs such as Fe-C, Ni-C and Co-C by irradiating nanosecond laser pulses into a metalocene-xylene solution under both room temperatures and normal atmospheric pressures. In their study, the resultant Co-C MNPs with well-ordered graphitic shells have a strong resistance in environmental degradation such as oxidation with air or dissolution in acids; it also shows soft ferromagnetic properties. The authors also discussed the growth mechanism, they declared that irradiation of the metalocene-xylene solution with a nanosecond pulse laser seem to lead the metal ions to agglomerate producing NPs. This agglomeration infers that the metal NPs enhance the laser energy absorption of the solution, resulting in an increase in the local temperature. At high temperatures, dissolution of the decomposed carbon from xylene may occur at the surface of metal NPs. Then, upon termination of the laser pulse, a rapid cooling of the solution containing metal NPs with the dissolved carbons will occur until the next pulse is fired. During each period between the pulses, carbons will be supersaturated on the surface of the metal core due to the reduction in the carbon's solubility around the metal core [114]; because of the rapid NP cooling, the supersaturated carbons stop growing, resulting in the production of the observed CEMNPs instead of carbon nanotubes [115]. To synthesize NPs by this process, it has been suggested that a nanosecond laser pulses at a high peak power plays an important role in the formation of a proper temperature field in the solution.

Due to the fact that the method is simple and can be operated under ambient conditions, it is expected that CEMNP synthesis could be scaled up relatively easily.

SOLID PHASE SYNTHESIS

Solid-phase approaches have been used for synthesis of CEMNPs. Examples are those based on high-temperature annealing of materials such as Fe_2O_3 plus C powders [116], elementary Fe plus C powders [117], and Co NPs plus copolymers [118]. However, the size and thus the magnetic properties of the final particles could hardly be controlled, and superparamagnetic particles could not be obtained as the starting particle size was usually much larger than 10 nm.

Combustion Synthesis

Combustion syntheses have been applied for the preparation of CEMNPs [106,119-120]. Martirosyan *et al*. produced cobalt ferrite, $CoFe_2O_4$, crystalline NPs (50-100 nm) by using the carbon combustion synthesis of oxides (CCSO) [120]. In their combustion synthesis process, the exothermic oxidation of carbons generate a thermal reaction wave that propagates through the solid reactants mixture of CoO and Fe_2O_3 converting it to cobalt ferrite. They found that the extensive emission of CO_2 increased the porosity and friability of the product. Also, a complete conversion to ferrite $CoFe_2O_4$ structure was obtained only for carbon concentrations exceeding 12 %wt. Solid state interactions between CoO and FeO with the growth of the crystalline cobalt ferrite particles started in the early period of the combustion and continued into the post combustion zone. As expected, the average particle size increased with increasing combustion temperatures.

Annealing

In order to overcome problems of relatively low productivity, the existence of complex phases, and the difficulty in separating CESNs from impurities in the gas-phase synthesis approaches, such as arc discharge and CVD, were recently proposed a synthesis of an Fe/C solid solution CEMNPs with a high controllability of chemical composition and particle size, by Wang *et al*. [121]. The unique feature of their approach is that CESNs can be prepared to have different sizes and thus different magnetic properties just by annealing a Fe-C solid solution at different temperatures. Also good is that heat treatment is at a low temperatures such as 600 °C, and the majority of the NPs have a size of about 8 nm also they are embedded in an amorphous carbon matrix. The materials that have such fine ferrous NPs show a superparamagnetic behaviour at room temperatures. However, after heat treatment at high temperatures such as 800 °C, most of the NPs have a size of about 30 nm and are encapsulated into graphitic carbon shells. The materials having such large ferrous NPs show a permanent magnetic behaviour at room temperatures.

Tokoro *et al*. by applying the annealing technique synthesized iron NPs with boron nitride (BN) and carbon (C) nanocoatings [122]. Mixtures of α-Fe_2O_3 and boron or carbon powders were employed as the starting materials they were annealed at temperatures above 1273 K in a nitrogen atmosphere.

The advantages of the solid-phase approach include a good controllability of the particle sizes, thus a good controllability of superparamagnetism; it generates of few impurities, and is suitable for large-scale production.

PROTECTION METHODS

MNPs are very sensitive to oxidation and agglomeration due to having a large specific surface area and are also high in its chemical reactivates as well as its magnetic dipole interaction. Under ambient conditions, rapid oxidation of the nanoparticles' surfaces occurs, leading to the creation of thin oxide layers that dramatically change the particle properties. Natural agglomeration of nanoparticles into larger clusters is another problem that hinders the processing of such materials. In order to preserve their specific magnetic properties, and to protect nanoparticles from both oxidation and agglomeration, the application of the encapsulation procedure has been proposed. Encapsulation of nanoparticles has been successfully employed by using carbon, silica, precious metals, metal oxides, organic polymers and surfactants.

The stability of a magnetic colloidal suspension results from the equilibrium between the attractive and repulsive forces. Stabilization and persevere from the agglomeration of magnetic particles can be achieved by playing on one or both of the two repulsive forces: electrostatic or steric repulsion.

Organic Coatings

Surfactants or polymers are often employed to passivate the surface of the nanoparticles during or after the synthesis to avoid agglomeration. Several approaches have been developed to coat MNPs, including *in situ* and/or after-synthesis with organic coatings. In the first approach, NPs are coated during the synthesis in this state, particle growth can be limited. For example, Josephson *et al*. have developed a co-precipitation process in the presence of dextran [124]. The post-synthesis coating method consists of grafting the polymer or surfactant onto the magnetic particles once synthesized [125-127].

Generally electrostatic repulsion or steric repulsion can be used to disperse nanoparticles and keep them in a stable colloidal state (stabilization of synthesized NPs in suspension). Also, surfactants or polymers can be chemically anchored or physically adsorbed on MNPs to form a single or double layer [128,129], which creates repulsive (mainly as steric repulsion) forces to balance the magnetic and the van der Waals attractive forces acting on the NPs. Thus, by steric repulsion, the magnetic particles are stabilized in the suspension.

Surfactants

A dense coverage by the organic surfactant is crucial to preventing the particles from being oxidized by air. Sun and Murray [130] have demonstrated the synthesis of Co nanoparticles in the presence of an organic surfactant such as oleic acid, lauric acid, trioctylphosphonic acid and pyridine. Among organic surfactants, oleic acid is an excellent capping agent that can bind strongly to the surface of metals with native oxides through the carboxyl group. It has been widely used in the synthesis of colloidal NPs for a large number of metals. Recently, Lu *et al*. [131] compared a number of surfactants (stearic acid, oleic acid and elaidic acid) for the synthesis of magnetic Co NPs for investigation of the difference between the capping agents in their ability to effect the controlling size, distribution and air stability of MNPs. They found that the poor performance of stearic acid on nanoparticles stability can be mainly attributed to its linear conformation. Unlike oleic or elaidic acid, there is no C=C double bonding in the chain of the stearic acid. They declared that the interaction of double bonding between olefinic acids could assist in the formation of a densely packed layer on the surface of Co NPs. The overlapping of double bonds between adjacent molecules would enhance the hardness of the capping layer. Since the densely packed surface layer is ‘‘harder’’ than those formed from aliphatic acids, the distance between adjacent particles will be precisely determined, allowing the particles to self-organize into ordered arrays. Also, due to the existence of double bond in olefinic acids, it is possible to form magnetic gels by polymerizing and cross-linking the double bonds during the evaporation of solvent.

Polymers

Up to now most studies have focused on the development of surfactant's coating, recently polymers that stabilize MNPs are receiving more and more attention. Polymers can increase repulsive forces more than surfactants. In addition, a polymer coating on the surface used for the designed purpose of a well-defined composite of materials and their dispersions offer a

high potential of application in several fields [132-135].

Two approaches have been developed to coat MNPs with polymers. In the first, an irreversible attachment of the macromolecular chains to the particle surface can be done by chemisorptions. The other approach, as an alternative strategy, the polymerization is initiated directly from the particle surface to give a higher number of end attached polymer chains. Poly (ethylene oxide) chains have been grafted onto a magnetite (Fe_3O_4) surface to give brush-like hybrid particles [136-138]. Surface-initiated polymerization has been applied to various polymerization methods, including radical [139], cationic [140], anionic [141], ring-opening metathesis [142] and ring-opening polymerization (ROP) [143-145].

In the literature, both natural and synthetic polymers have been used for coating of MNPs. The most common natural polymers are dextran, chitosan, starch, gum arabic, and gelatine. Also, The most common synthetic polymers are polyethylene glycol (PEG), polyvinyl alcohol (PVA), poly lactide acid (PLA), alginate, polyacrylic acid (PAA) and polymethylmethacrylate (PMMA).

A thin polymer coating is not very suitable to protect extremely reactive MNPs. Metallic MNPs, stabilized by single or double layers of surfactants or polymers are not air stable, making them easily leached by an acidic solution [146], resulting in the loss of their magnetization. Another drawback of polymer-coated MNPs is the relatively low intrinsic stability of their coating at higher temperatures, a problem which is even more enhanced by the possible catalytic action of the metallic cores. Therefore, the development of other methods for protecting MNPs against deterioration is of great importance.

Inorganic Coatings

Metal oxides. A very simple approach to protect the magnetic particles is to induce a controlled oxidation of a pure metal core, a technique long known for the passivation of air-sensitive supported catalysts. Bönnemann *et al*. [147] developed a mild oxidation method, using synthetic air to smoothly oxidize the outer surface of the synthesized cobalt nanoparticles to form a stable CoO which can stabilize the cobalt nanoparticles against further oxidation. When iron NPs are exposed to aqueous solutions, immediately a shell which consists of mostly iron oxides and hydroxides will form on the outer surface of the iron core which can stabilize the iron NPs against further oxidation. Thus iron NPs exhibit characteristics of both iron oxides (*e.g.*, as a sorbent) and metallic iron (*e.g.*, as a reductant) which can be very useful in application [148]. Recently, Peng and Sun [149] found that Fe NPs are not chemically stable, and when exposed to air due to oxidation give core-shell Fe-Fe_3O_4 structures with both Fe and Fe_3O_4 in the amorphous state. In their study, controlled oxidation of the core-shell of the NPs in the presence of the oxygen-transfer reagent trimethylamine N-oxide (Me_3NO) led to the formation of an intermediate core-shell-void Fe-Fe_3O_4, and furthermore to hollow Fe_3O_4 NPs.

Another way for protection of MNPs via metal oxides coating, is using metal oxides with different natures in respect to the magnetic core. For this purpose up to date, metal oxides such as titanium oxide [150], zirconium oxide [151] and aluminum oxide [152-155] have been used as coatings for magnetic iron oxide nanoparticles. The surfaces of these metal oxides are readily modified with phosphorylated molecules which can be very useful for biological applications [154]. Among these metal oxides, the selectivity of alumina-coated magnetic iron oxide NPs toward phosphorylated molecules is superior to that of those coated with titania [156] and such complexes are stable within a large range of pH values [157].

Precious metals. Gold is a widely used coating material due to its specific surface derivative properties for subsequent treatment with chemicals or biomedical agents. For example, it is well established that Au NPs surfaces could be functionalized with thiolated organic molecules for further applications [158,159]. The most common techniques for deposition of precious metals on MNPs are reactions in microemulsion [160,161] and redox transmetalation [162-164], to protect the cores against oxidation.

Cheon *et al*. [162] reported the synthesis of platinum-coated cobalt by refluxing cobalt NPs (*ca*. 6 nm) and [Pt-$(hfac)_2$] (hfac = hexafluoroacetylacetonate) in a nonane solution containing $C_{12}H_{25}NC$ as a stabilizer. After 8 h reflux and the addition of ethanol and centrifugation, the colloids are isolated from the dark red-black solution in their powder form. These methods are not able to maintain the morphology of the magnetic core particles and are time-consuming. Recently, Wu *et al*. reported [165] a simple, rapid and feasible route to prepare air-stable magnetic Fe_3O_4/Au NPs by sonolysis of a

solution mixture of hydrogen tetrachloroaureate (III) trihydrate ($HAuCl_4$) and (3-aminopropyl) triethoxysilane (APTES)-coated Fe_3O_4 NPs with the further drop-addition of sodium citrate. A diamagnetic layer formalized the shell that could potentially reduce magnetic properties of the magnetic core of the nanoparticle. At the same time, it is expected that magnetite nanoparticles can be passivated to avoid oxidation by diamagnetic layer coating without significant effects on their magnetic properties. In their study, superconducting quantum interference device (SQUID) magnetometry revealed that overlaying Fe_3O_4 NPs surfaces with a shell of Au had a negligible decrease on their magnetic behaviours.

Sun *et al*. [166] also showed that gold coating preserves the magnetic property of the iron core while enhancing its stability. They experimentally and for the first time theoretically investigated that the gold-coated iron oxide particle can selectively bind with sulphur-containing amino acids. Thus, the combination of magnetism, selectivity and stability displayed in gold-coated iron oxide particles makes it very promising in applications such as magnetic separation, controlled release, and targeted drug delivery.

Silica. Magnetic microspheres consisting of a magnetic core and silica shell have attracted particular attention [167,168] for their unique magnetic responsivity, low cytotoxicity, easy chemically modifiable surfaces and the easy control of interparticle interactions, both in solutions and within structures, through the variation of the shell's thickness. Silica coating made the sol anionic across the working pH range. The stable negative charge in the pH ranges from 6-7 is desirable because this mimics the negative charge of most biomolecules in physiological conditions [169]. Also, silica coatings have high stability under aqueous conditions (at least if the pH value is sufficiently low). Zhao *et al*. [170,171] found that silica can be a good coating for the prevention of oxidation of pure Fe_3O_4 and it easily loses its magnetism when the pH is below 4.0.

Two different approaches have been explored to generate silica coatings on the surfaces of iron oxide particles. The first method relied on the well-known Stöber process [172], in which silica was formed *in situ* through the hydrolysis and condensation of a sol-gel precursor. The other method was based on microemulsion synthesis [62,173], in which micelles or inverse micelles were used to confine and control the coating of silica on the core NPs. This method might require greater effort to separate core-shell NPs from the large amount of surfactants associated with the microemulsion system.

Core-shell magnetic mesoporous silica microspheres with strong magnetic responsivity, orientated and accessible mesopores and high dispersibility are highly valuable. Sen *et al*. [174] reported the template-assisted fabrication of magnetic mesoporous silica-magnetic nanocomposite and its potential for application in magnetic bioseparation. They observed that the surface area for silica-magnetite nanocomposite is 10 times greater than the magnetite core (increase from 25 $m^2\ g^{-1}$ to 250 $m^2\ g^{-1}$). Very recently, Deng *et al*. [175] developed a new approach for preparation of core-shell magnetic mesoporous silica microspheres ($Fe_3O_4@n SiO_2@m SiO_2$). TEM images of the preparation steps are shown in Fig. 4. The unique microstructure of the obtained microspheres would be very useful for many applications. First, the middle nonporous silica layer could protect the magnetite from etching in harsh application occasions. Second, the mesoporous silica shell not only offers a high surface area (365 $m^2\ g^{-1}$) for the derivation of numerous functional groups but also the shell provide large accessible pore volume for the adsorption and encapsulation of biomacromolecules and even functional nanoparticles (*e.g.*, quantum dots). Third, the obtained microspheres posses' superparamagnetism with a high magnetization (53.3 emu g^{-1}), is notably due to their unique perpendicular orientation. The mesopore channels of the microspheres are readily accessible, favoring the adsorption and release of large guest objects triggered by external stimulus.

In the case of silica-coated MNPs, it is difficult or impossible to achieve a fully dense and nonporous silica coating, thus making difficult the maintaining of a high stability of these NPs under harsh conditions, especially in basic environments.

Carbon. Carbon encapsulated MNPs (CEMNPs) have received considerable attention in recent years because of their potential as small magnetic clusters for high density magnetic data storage, in ferrofluid applications, magnetic resonance imaging and so on [176].

Carbon is one of the best solutions for encapsulation of metal NPs because carbon is more chemically and thermally stable, cheap, light and biocompatible. In addition, the carbon shell can be thinned/removed by hydrogen or oxygen gas

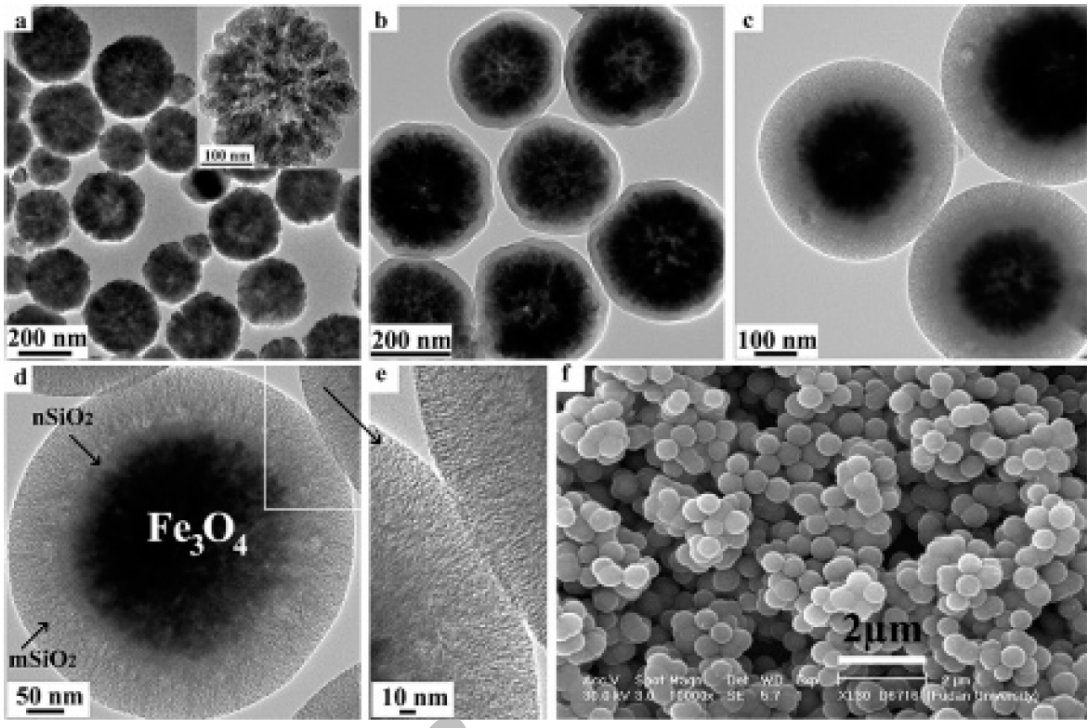

Fig. 4. TEM images of (a) Fe_3O_4 particles, (b) Fe_3O_4@$nSiO_2$, (c-e) Fe_3O_4@$nSiO_2$@$mSiO_2$ microspheres and (f) SEM image of Fe_3O_4@$nSiO_2$@$mSiO_2$ microspheres [175].

when so desired. Owing to these advantages of carbon, the various methods for preparing the carbon capsulated NPs have been developed actively, such as arc discharge techniques, chemical vapor depositions, combustion, pulse laser decomposition and pyrolysis of metal complexes.

Interest in carbon-metal systems is due to the possibility of obtaining nanocrystalline metal particles encapsulated by crystalline or amorphous carbon. Park *et al*. [113] tested the chemical stability of CEMNPs by sonicating in a 10 M HCl solution using an ultrasonic cleaner. After ultrasonication, no CEMNPs with imperfect carbon shells, *e.g.*, amorphous carbon coated Fe-C nanoparticles about 200-300 nm in size, were found in the HR-TEM observation. Conversely, CEMNPs with graphitic layers were still found in the HR-TEM images. They concluded that graphitic coatings have better chemical stability in acids at least in respect to amorphous coating. Genererally, low graphitization of the carbon shell is observed at low laser energy conditions, which is considered to be due to the relatively low solution temperature. Thus, in recent years Fe, Ni and Co have received more attention in CEMNPs synthesis due to their ferromagnetic properties; also their unique catalyzing ability in the transformation of amorphous carbon into graphitic carbon at sufficiently high temperatures [177].

STRATEGIES TO FUNCTIONALIZATION

Particle interactions with their environment are greatly affected by their surface functionality. Development of methods aimed at the postsynthetic surface modification of MNPs is important to render them chemically functional and to control their solubility; also the large application of MNPs in different fields renders their environmental effects highly important. Most applications require the NPs to be chemically stable, uniform in size, and possessing the ability of well-dispersion in liquid medias. The surface of MNPs should be modified with suitable functional groups or molecules. The electrostatic chimio-adsorption and covalent conjugation

strategies have been used for surface functionalization of MNPs.

There are two general approaches in nanoparticles surface functionalization: ligand addition and surface ligand exchange [178,179]. In ligand addition, incoming ligands have added a double-layer like structure to the original ligands which cover the surface of the synthesized MNPs. In ligand exchange the original ligand are replaced with a new bifunctional ligand with one functional group capable of binding to the particle surface via a strong chemical bonding and the other group can be used for further functionalization of MNPs.

Biological Aspects

For biomedical applications and bioanalysis, the ability to solubilize the NPs in water and to modify their surfaces with molecules, proteins, oligonucleotides, or other targeting agents, is a crucial step towards their widespread use. Conversely, materials applications magnetic particle will likely require a broad range of chemical functionalization and solvent compatibility.

Because of the potential benefits of multimodal functionality in biomedical applications, researchers would like to design and fabricate multifunctional MNPs. Currently there are two strategies to fabricate magnetic nanoparticle-based multifunctional nanostructures. The first is, molecular functionalization involving the attachment of antibodies, proteins and dyes to MNPs. The other method integrates the MNPs with other functional nanocomponents, such as quantum dots (QDs) or metallic NPs. Because they can exhibit several features synergistically and deliver more than one function simultaneously, such multifunctional MNPs could have unique advantages in biomedical applications. Gao *et al*. [180] recently reviewed examples of the design and biomedical application of multifunctional MNPs.

On other hand, to take advantage of their high-quality properties in biological applications, it is necessary to transfer MNPs from an organic to an aqueous solution. Some groups have reported surface modification techniques including surface exchange with cyclodextrin (CD) [181,182], copolypeptides [183] and intercalation of surfactants [184]. Especially, some reports have given prominences to surface exchange with dimercaptosuccinicacid (DMSA) by which modified iron oxide NPs are fairly stable in water over wide ranges of pH and salt concentrations [185-190], which makes them preferable in biological applications.

Catalysis Aspects

Catalysts supported on MNPs, usually iron oxides, can be quickly and easily recovered in the presence of an external magnetic field for reuse. In addition, internal diffusion limitations can be avoided, because all of the available surface areas of the nonporous MNPs are external. The surface of MNPs can be functionalized to accommodate a wide variety of organic and organometallic catalysts. For example, Dálaigh *et al*. [191] developed the first magnetic NPs-supported 4-N,N-dimethylaminopyridine (DMAP) analogue, for use as a robust heterogeneous nucleophilic catalyst with unprecedented activity and recyclability. Also, Hu *et al*. [192] designed novel magnetite NPs supported by chiral Ru complexes [Ru (BINAP-PO_3H_2)(DPEN)Cl_2]) that catalyze heterogeneous asymmetric hydrogenation of aromatic ketones with remarkably high activity and enantioselectivity.

Extraction and Removal Aspects

Although, sometimes the pure MNPs can be used in extraction and removal of inorganic pollutants without the need for further functionalization, generally it is needed to modify the surface of synthesized MNPs for attachment of some functional groups in target application purposes. Hu *et al*. [193] employed magnetic Fe_2O_3 nanoparticles as an adsorbent for the removal and recovery of Cr(VI) from wastewaters, and the adsorption capacity was found to be very high. However, it should be pointed out that pure inorganic NPs (such as Fe_3O_4 and Fe_2O_3 NPs) can easily form large aggregates, which may alter their magnetic properties [194]. Moreover, these nanometer-sized metal oxides are not target-selective and are unsuitable for samples with complicated matrices [195]. The modification of these MNPs with a suitable coating has been proven to be one of the most efficient ways [196]. Therefore, preparation of modified MNPs for selective extraction or removal of organic or inorganic pollutants is a requirement for future functionalization of particles with suitable reagents which have functional groups such as COOH, NH_2, and SH. For example, White *et al*. [197] immobilized poly-l-cysteine (PLCysn) onto the surface of magnetic γ-Fe_2O_3 NPs, and used

it as a selective heavy metal chelator. They found that for As(III), Cu(II), Ni(II) and Zn(II), the binding capacities were higher than the metal adsorption capacities of the unfunctionalized particles. Up to date different reagents have been used for functionalization of MNPs for extraction and removal proposes, some of them are presented on Tables 1, 2 and 3.

CHARACTERIZATION COMMON TECHNIQUES

Magnetic properties and various applications of MNPs depend highly on size, morphology, structure and the surface functional groups of the prepared NPs. Therefore, up to date various characterization techniques have been used for this purpose.

Size and Morphology

TEM and HR-TEM. Transmission electron microscopy (TEM) is routinely used in the determination of particle core size. This technique reports the total particle size of the core (crystalline and amorphous parts) and gives access to a number-weighted mean value. Furthermore, it provides details on the size distribution and the shape (Fig. 4). However, this technique needs an analysis by image treatment, and must be performed on a statistically significant large number of particles.

High-resolution transmission electron microscopy (HR-TEM) gives access to the atomic arrangement. It can be used to study local microstructures (such as lattice vacancies and defects, lattice fringe, glide plane, or screw axes) and the surface atomic arrangement of crystalline NPs [198].

SEM. Scanning electron microscopy (SEM) is a widely used technique for the determination of morphology and size distribution of prepared particles in the scales of micro to nano range. SEM is not a good technique for characterization of core/shell NPs because this technique reports total particle size (Fig. 4). Resolution of the SEM is lower than TEM and it is not efficient for NPs with particles size lower than 20 nm.

PCS. Photon correlation spectroscopy (PCS), also called dynamic light scattering (DLS), is a common technique to obtain NPs size. The determination of the diffusion coefficient of the nanoparticles in solution gives access to the hydrodynamic radius of a corresponding sphere and the polydispersity of the colloidal solution [199].

Structure and Elemental Analysis

EDXD. Energy dispersive X-ray diffraction (EDXD) provides the advantage of being carried out on the suspension and is used to improve the knowledge of fine structural details. EDXD can be used to provide an elemental analysis and determination of the chemical composition of prepared magnetic NPs. From EDXD data, the ratio of the elements in the NPs structure can be estimated.

XRD. The XRD spectra is used for determining the crystallographic identity of the produced material, phase purity

Table 1. Application of Magnetic Nanoparticles for Removal of Organic Compounds

Matrix	Analyte	Adsorbent	q_{max}	Ref.
Aqueous solutions	Crocein orange G and acid green 25	Carboxymethylated chitosan-conjugated Fe_3O_4 nanoparticles	1883 and 1471 mg g^{-1}	[269]
Karoon river water	Amaranth	Iron oxide nanoparticles coated with cetyltrimethylammonium bromide	1.05 mg mg^{-1}	[270]
0.03 M Phosphate buffer	Methylene blue	Polyacrylic acid-bound iron oxide MNPs	0.199 mg mg^{-1}	[271]
Distillate water	Acid orange 10	3-Aminopropyltriethoxysilane modified magnetic silica and 3-aminopropyltri-ethoxysilane modified silica	61.33 and 48.98 mg g^{-1}	[272]
0.03 M phosphate buffer	*Candida rugosa* lipase	Polyacrylic acid-coated magnetic nano-adsorbent	0.605 mg mg^{-1}	[273]

Table 2. Some Recent Applications of Magnetic Nanoparticles for Removal of Metal Ions

Matrix	Analyte	Adsorbent	q_{max} [b]	Removal%	pH_{sample}	Ref.
Water and blood	UO_2^{2+}	Bisphosphonate dopamine derivative-conjugated Fe_3O_4 NPs	a	99 and 69	pH ~ 5	[274]
Water and blood	Pb^{2+}	4,4-Difluoro-4-bora-3a,4adiaza-s-indacene (BODIPY) derivative-Ni@SiO_2 NPs	a	97 and 96	pH 7	[275]
Aqueous solution	Cr(VI)	Montmorillonite-supported Fe_3O_4 NPs	15.3 mg g^{-1}	a	pH 2.0-2.5.	[276]
Water samples	Hg(II), Pb(II), Cd(II) and Cu(II)	Humic acid coated Fe_3O_4 NPs	46.3-97.7 mg g^{-1}	95-99	pH 6.0	[277]
Water samples	Cu^{2+}	Naked Fe_3O_4 NPs and Gum arabic modified Fe_3O_4 NPs	17.6 and 38.5 mg g^{-1}	a	pH 5.1	[278]
Water samples	Cr(VI)	$MnFe_2O_4$, $MgFe_2O_4$, $ZnFe_2O_4$, $CuFe_2O_4$, $NiFe_2O_4$, $CoFe_2O_4$. NPs	a	20-99.5	pH = 2	[279]
Water samples	As(III), Cd(II), Cu(II), Ni(II), Pb(II) and Zn(II)	Poly-l-cysteine functionalized γ-Fe_2O_3	71-681 μmol g^{-1}	a	pH 7.0	[198]
		Unfunctionalized γ-Fe_2O_3	90-522 μmol g^{-1}			
Wastewater	Ni(II)	Alginate microcapsules containing Cyanex 272 (as extractant) and γ-Fe_2O_3	0.52 mmol g^{-1}	70	pH 8.0	[280]
Aqueous solutions	Cu(II) and Cr(VI)	Amino-functionalized PAA-coated Fe_3O_4 NPs with DETA	12.43 and 11.24 mg g^{-1}	a	pH 5 and 2	[281]
Different water samples	Hg, Ag, Pb, Cd, and Tl	Dimercaptosuccinic acid functionalized Fe_3O_4 NPs	227 mg g^{-1} (Hg)	a	a	[282]
Wastewater	Cr(VI)	Maghemite	19.2 mg g^{-1}	a	pH of 2-3	[194]
Aqueous solutions	Cu^{2+}, Ni^{2+}, Zn^{2+}	3-Aminopropyltriethoxysilane functionalized mesoporous Fe_3O_4 NPs	a	a	2 > pH < 6	[283]

[a]Data not reported: [b]Maximum sorbent capacity.

Table 3. Recent Applications of Magnetic Nanoparticles as SPE Sorbents for Preconcentration and Determination of Organic and Inorganic Compounds after Elution Target Analytes from the Surface of the Sorbents

Matrix	Analyte	Adsorbent	Detection system	DL	V_{sample} (ml)	EF	DLR	Eluent	RSD (%)	Ref.
Environmental water samples	Typical phenolic compounds	CTAB or CPC coated Fe_3O_4 NPs (mixed hemimicelles)	HPLC-FL	12-34 ng l^{-1}	800	800	a	6 ml of acetonitrile	2-7	[170]
Environmental water samples	Typical phenolic compounds	CTAB or CPC coated Fe_3O_4/SiO_2 NPs (mixed hemimicelles)	HPLC-FL	7-20 ng l^{-1}	800	1600	0.1-30 µg l^{-1}	3 ml (3 × 1) acetonitrile containing 1% acetic acid	-	[171]
Environmental water samples	Typical chlorophenols	CTAB coated Fe_3O_4 NPs (mixed hemimicelles)	HPLC-UV	0.11-0.15 µg l^{-1}	700	700	0.5-50 µg l^{-1}	4.5 ml (3 × 1.5 ml) methanol	4.8-5.9	[323]
Environmental water samples	Trimethoprim	SDS coated Fe_3O_4/Al_2O_3 NPs (mixed hemimicelles)	HPLC-UV	0.09 µg l^{-1}	500	1000	0.24-30 mg l^{-1}	3 ml (3 × 1) methanol	< 6	[324]
Environmental water samples	Polycyclic aromatic hydrocarbon	C_{18} functionalized Fe_3O_4/SiO_2 NPs	GC-MS	0.8-36 µg l^{-1}	20	a	10-800 µg l^{-1}	*n*-hexane (3 × 1.5 ml)	< 10	[325]
Cigarettes samples	Ergosterol	C_{18} functionalized Fe_3O_4/SiO_2 NPs	GC-MS	0.01 mg l^{-1}	1.0	a	0.1-10 mg l^{-1}	*n*-hexane (0.1 ml × 3)	< 4.1	[326]
Water samples	Triazines	Bilayer decanoic acid coated Fe_3O_4 NPs	HPLC-ESI-MS/MS	10-30 ng l^{-1}	400	a	0.03-50.0 µg l^{-1}	2 ml HCl solution (10 M)	2.3-3.7	[328]
Karoon River water sample	Basic fuchsin	SDS coated Fe_3O_4 NPs	UV-Vis	7.3 µg l^{-1}	50	40	10-300 µg l^{-1}	2.5 ml 70% methanol in 1 M acetic acid	< 4.73	[329]
Seawater samples	Te(IV)/ Te(VI)	Silica-coated Fe_3O_4 NPs modified with γ-mercaptopropyltrimethoxysilane	ICP-MS	0.079 ng l^{-1}	160	320	a	0.5 ml of mixed solution of 0.03 M $K_2Cr_2O_7$ in 2.0 M HCl	7.0	[330]
Biological and environmental samples	Cd, Cu, Hg, and Pb	Silica-coated Fe_3O_4 NPs modified with γ-mercaptopropyltrimethoxysilane	ICP-MS	24-107 pg l^{-1}	250	413-476	a	0.5 ml of 1 M HCl and 2% (m/v) thiourea	3.7-9.6	[331]
Environmental samples	Cr, Cu and Pb	Bismuthiol-II-immobilized Fe_3O_4/SiO_2 NPs	ICP-OES	43-85 ng l^{-1}	100	87-96	a	1 ml of 1 M HNO_3	3.5-4.6	[332]
Water samples	Fluoride	Magnetic iron oxide nanoparticles	UV-Vis	0.015 µg ml^{-1}	250	50	0.04-1.25 µg ml^{-1}	2 ml of 1.0 M NaOH	< 3.5	[333]

[a]Data not reported.

and for calculating the mean particle size based on the broadening of the most prominent peak in the XRD profile. Scherrer's [200] equation:

$$D = K\lambda/\beta \cos\theta \quad (6)$$

is used to calculate the average particle diameter D (in Å), where θ is the angle of the peak, β is the width at half maximum (FHWM) of the respective XRD peak, λ is the X-ray radiation wavelength in ångströms (Å) and K is a constant which is very close to unity and is related both to the crystallite shape and to the way in which β and D are defined. The broadening of the diffraction peaks is related to the small particle size.

In addition, in a diffraction pattern, the intensity can be used to quantify the proportion of magnetic nanoparticles formed in a mixture by comparing experimental peaks and reference peak intensities [201].

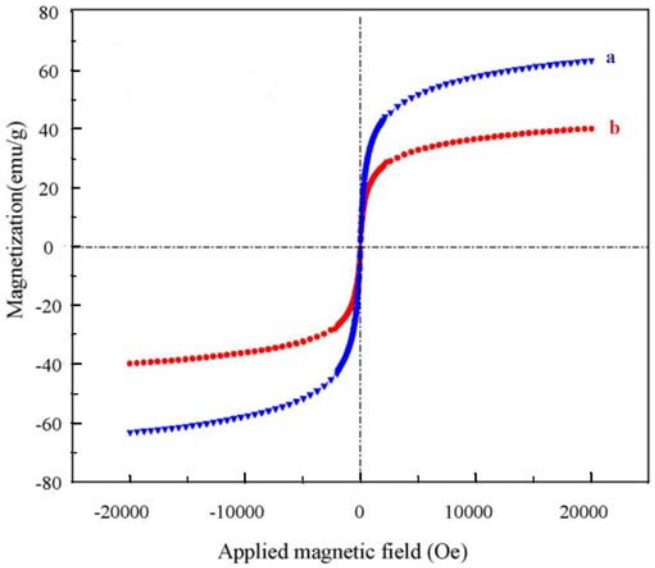

Fig. 5. VSM magnetization curves of Fe_3O_4 NPs (a) and Fe_3O_4/SiO_2 NPs (b) [171].

Magnetic Properties

Many techniques are available to measure the magnetic properties of an assembly of MNPs. SQUID magnetometry [202] and vibrating sample magnetometry (VSM) [203] are powerful tools to measure the sample's net magnetization. Like most conventional magnetization probes, both techniques are not element specific but they rather measure the whole magnetization.

VSM. VSM is used to evaluate magnetization of the MNPs as a function of an applied external magnetic (H) generally between -3 and 3 Tesla. Based on the obtained VSM curve at low and room temperatures, magnetic behaviour of the MNPs can be identified. For example at room temperature, the zero magnetic remanence (when H is zero), and the anhysteretic loop feature indicates that the MNPs are superparamagnetic. Also, from the plateau part of the VSM curve, saturation magnetization (M_s) can be determined. On the other hand, it is most important that the core/shell materials should possess sufficient magnetic and superparamagnetism properties for use in practical applications; VSM is a good technique for estimating a shell's effect on M_S. For examples, Zhao *et al.* [171] applied the VSM technique for estimating the silica cell effect on the M_S of Fe_3O_4 NPs (Fig. 5).

SQUID. SQUID magnetometry is routinely used to assess these magnetic properties. Monitoring magnetization as a function of temperature for particles cooled with or without an applied magnetic field followed by warming particles in the presence of a magnetic field allows the characteristic blocking temperature to be determined.

Surface Characterization

X-Ray photoelectron spectroscopy (XPS). XPS is a very useful technique for the study of the mechanisms of the reaction that occurs on the surface of MNPs. The XPS spectra are very useful in the determining of the characteristics in the bonding of the different elements involved. Also, it can be applied to confirm the structure as well as in the speciation of elements which are in the chemical composition MNPs. Karabelli *et al.* [204] applied the XPS technique for investigation of the uptake mechanism of Cu^{2+} by using zero-valent iron. In their study, XPS investigations indicated that Cu $2p_{3/2}$ lines are centered at a binding energy of 932.3 ± 0.1 eV. Based on the binding energy of Cu^0 and Cu^+, and by calculating the Auger parameter they found the valence state of Cu under analysis. The calculated Auger parameter indicated that the recorded signal was derived mainly from Cu^+ rather than Cu^0. This result was also confirmed by XRD patterns recorded by the iron nanoparticles at the end of the

uptake process. XRD analysis showed the appearance of more intense cuprite, Cu_2O, signals compared to metallic copper, Cu^0, signals. They declared that the primary uptake mechanism is of the redox type.

Also, Gao *et al*. [205] applied the XPS technique to confirm the chemical structure of the prepared magnetite NPs. In their study, the XPS spectra of the products showed that the binding energies relating to $Fe2p_{3/2}$, $Fe2p_{1/2}$ and O1s are about 711, 725 and 531 eV, respectively. The data are consistent with the values reported for Fe_3O_4 in literature [206]. Therefore, XPS data together with XRD results prove the composition and structure of the product.

Zetasizer. The **c**haracterizing of a particle's surface properties is necessary in the understanding and for the predicting of properties under physiological conditions and also to optimize conjugation chemistry. Surface charge is characterized by zeta (ζ) potential analysis. The isoelectric point, also referred to as PZC (point of zero charge), is the pH at which the particles in suspension have a net charge of zero and no mobility in the electric field, Fig. 6 shows the effect of silica cells surface charge of the magnetite cores.

FT-IR. FT-IR spectroscopy is a useful tool for the understanding of the functional group of any organic molecule. FT-IR has been widely used to confirm an attachment of different functional groups in each step of functionalization. For example, Grass *et al*. [207] applied IR spectroscopy for the characterization of carbon-coated cobalt NPs before and after functionalization with a chlorobenzene group. The IR spectrum of the chloro-functionalized magnetic nanobeads strongly differs from that of the untreated carbon-coated magnetic beads and shows peaks characteristics of a 4-substituted chlorobenzene group. This is supported by the good match with the IR spectrum of chloro-4-ethyl-benzene and the deviation from that of chlorobenzene. This observation rules out the possible physisorption of chlorobenzene on the graphite surface.

Thermal gravimetric analysis (TGA). TGA has been performed to confirm the coating formation (especially surfactants or polymers) to estimate the binding efficiency on the surface of MNPs. Shen *et al*. [49] used TGA measurements to confirm the existence of two distinct populations of surfactants coated on the iron oxide surface. In their study, for all bilayer surfactant-coated particles (C_{10}/C_9-C_{13}), the heating curves are characterized by mass losses with two distinct steps, revealing a different pattern from that observed for monolayer surfactant-coated particles. Also, to evaluate the surfactant packing density, the mass losses assigned to certain fractions of the surfactant coatings. For bilayer surfactant-coated particles, the weight reductions for the first and second steps are attributed to the quantitative mass losses of the outer (secondary surfactant) and inner (primary surfactant) layers of the coating, respectively.

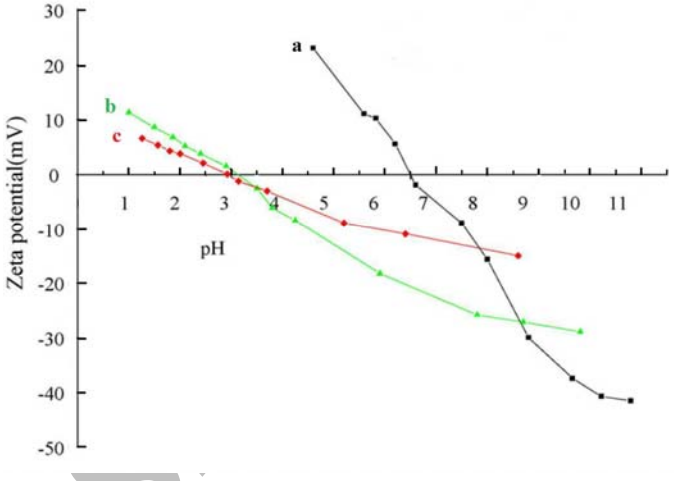

Fig. 6. Zeta-potential of Fe_3O_4 NPs (a), Fe_3O_4/SiO_2 NPs (b) and native silica (c) [171].

Other Techniques

Field flow flotation. Because of the difficulty of synthesizing monodisperse particulate materials, a technique capable of characterizing the magnetic properties of polydisperse samples of MNPs is of great importance. Magnetic field flow fractionation (MFFF), separates species on the basis of their magnetic susceptibility and is applicable to materials which have sizes from nanometres to micrometers [208,209]. Shown schematically in Fig. 7, MFFF causes the sample injected into a capillary to interact with an external magnetic field gradient that forces it toward the accumulation wall (*i.e.*, higher field strength). Material that interacts strongly with the field are restricted to the slower flow streams near the walls of the channel, while materials that interact weakly are free to experience the faster flow streams towards

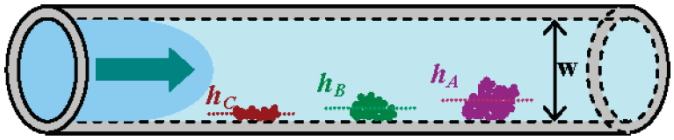

Fig. 7. Diagram of magnetic particle separation in capillary MFFF, weakly interacting particles having a larger average layer thickness (h_A) and elute at shorter times; strong interaction results in the smallest layer thickness (h_C) [210].

the center of the channel. Latham *et al*. [210] for the first time demonstrate successfully the implementation of MFFF to separate and purify magnetic nanoparticle samples by capillary column.

APPLICATIONS

Industrial Applications

Magnetic encapsulates may find very important applications in various branches of high-tech industry, and also in many areas of everyday life. These potential applications include high density magnetic data storage devices, magnetic information storage, xerography, electronics (recording media), catalysis, magnetic inks (for jet printing), magnetic refrigeration and their systems *etc*. Therefore such materials are interesting from both the point of the fundamental study of materials science as well as their applications [211-218].

Magnetite and hematite have been used as catalysts for a number of industrially important reactions, including the synthesis of NH_3 (the Haber process), the high temperature water gas shift reaction, and the desulfurization of natural gas. Other reactions include the dehydrogenation of ethyl benzene to styrene, the Fishere-Tropsch synthesis for hydrocarbons, the oxidation of alcohols, and the large scale manufacture of butadiene [28].

All three forms of magnetic iron oxide are commonly used as synthetic pigments in paints, ceramics, and porcelain [219]. They possess a number of desirable attributes for these applications because they display a range of colors with pure hues and high tinting strength. They are also extremely stable and highly resistant to acids and alkalis. Pigments based on hematite are red, those based on maghemite are brown, and magnetite-based pigments are black [220]. These pigments are widely used in water-repellent stains for wood as they enable the wood grain to be seen while still providing protection against the damaging effects of sunlight. Pigments made from magnetite are also used in magnetic ink character recognition devices, and superparamagnetic magnetite particles are used in metallography for detecting flaws in engines.

In magnetic encapsulates, despite the apparent suppression of magnetization, encapsulation is critical in reducing inter-particle interactions. These interactions increase the probability of progressively losing the alignment of the ferromagnetic moments of particles placed in close proximity. This is undesirable in recording media applications where a natural separation would help to safely attain the highest possible packing density to obtain media with lower cost per bit of information and to improve the signal to noise ratio [107].

Biological Applications

Two key factors play an important role for *in vivo* applications of these particles: size and surface functionality. Even without targeting surface ligands, superparamagnetic iron oxide NPs (SPIOs) diameters greatly affect *in vivo* biodistribution. Particles with diameters of 10-40 nm, including ultra-small SPIOs (USPIOs), are optimal for prolonged blood circulation, they can cross capillary walls, and are often phagocytosed by macrophages which traffic to lymph nodes, and bone marrow [221].

Drug Delivery

Drug targeting has emerged as one of the modern technologies for drug delivery. The possibilities for the application of iron oxide magnetic nanoparticles (IOMNPs) in drug targeting have drastically increased in recent years [23, 24,26]. MNPs in combination with an external magnetic field and/or magnetizable implants allow the delivery of particles to the desired target area and fixes them at the local site while the medication is released and acts locally (magnetic drug targeting) [23,222,223]. Transportation of drugs to a specific site can eliminate side effects and also reduce the dosage required. The surfaces of these particles are generally

modified with organic polymers and inorganic metals or oxides to make them biocompatible and suitable for further functionalization by the attachment of various bioactive molecules [224].

For example, Banerjee *et al*. [182] recently prepared a novel magnetic drug carrier. They found that grafting CD molecules on the gum arabic (GA)-modified MNPs may lead to a drug carrier that possesses the following properties: (1) allows a controlled release of a bioactive substance; (2) can form noncovalent inclusion complexes with a wide variety of lipophilic drug molecules allowing the solubilization, stabilization, and transport of hydrophobic drugs; and (3) can be magnetically guided to the local site at the specified time for dosage and elimination.

Bioseparation

In biomedical research, separation of specific biological entities (*e.g.*, DNAs, proteins, and cells) from their native environment is often required for analysis. Superparamagnetic colloids are ideal for this application because of their on-off nature of magnetization with and without an external magnetic field, enabling the transportation of biomaterials with a magnetic field. In a typical procedure for separation, the biological entities are labeled by superparamagnetic colloids and then subjected to separation by an external magnetic field [23].

Nanometer-sized magnetic particles, such as superparamagnetic iron oxide particles, have been extensively used for separation and purification of cells and biomolecules in bioprocesses [23,24,26,225-227]. Due to their small size and high surface area, MNPs have many superior characteristics for these bioseparation applications compared to those of the conventional micrometer-sized resins or beads, such as good dispersability, the fast and effective binding of biomolecules, and reversible and controllable flocculation. Very recently, Xu and co-workers synthesized nickel-nitrilotriacetic acid (Ni-NTA) complex-conjugated MNPs and reported their excellent performance in manipulating histidine-tagged (His-tagged) proteins [228,229].

Hsiao *et al*. [230] designed C18-functionalized Fe_3O_4 nanoparticles not only to specifically trap phosphopeptides, but also nonphosphorylated peptides, both of which can be subsequently desorbed selectively by stepwise elution with different eluents and directly for MALDI-MS analysis without an elution step. Sen *et al*. [231] prepared mesoporous silica-magnetite nanocomposite and applied it to the extraction of sheared salmon sperm DNA. They declared that the binding mechanism of DNA on the surface of the nanocomposite is most likely to be due to electrostatic interactions between the negatively charged phosphate backbones of DNA with the positively charged surface of NPs in the physiological pH in the presence of high salt concentrations [232].

One of the trends in this subject area, is magnetic separation using antibodies to provide highly accurate the antibodies that can specifically bind to their matching antigens on the surface of the targeted species. For example, immunospecific, Liu *et al*. [233] prepared pigeon ovalbumin-bound $Fe_3O_4@Al_2O_3$ MNPs (POA-$Fe_3O_4@Al_2O_3$ NPs) for affinity capture of uropathogenic Escherichia coli.

Magnetic Resonance Imaging

At the boundary between nanomaterials and medical diagnostics, superparamagnetic iron oxide NPs are proving to be a class of novel probes useful for *in vitro* and *in vivo* cellular and molecular imaging. The face-centered cubic packing of oxygen in maghemite/magnetite, γ-Fe_2O_3/Fe_3O_4, allows electrons to jump between iron ions occupying interstitial tetrahedral and octahedral sites, thus giving the molecules half-metallic properties that are suitable for magnetic resonance imaging (MRI) [234].

Superparamagnetic contrast agents have an advantage of producing an enhanced proton relaxation in MRI in comparison with paramagnetic ones. Consequently, less amounts of a SPIO agent is needed to dose the human body than a paramagnetic one. To apply the magnetic fluids to a MRI contrast agent, a SPIO should be dispersed into a biocompatible and biodegradable carrier. Recently, Muller and co-workers [26] comprehensively reviewed applications of superparamagnetic iron oxide NPs as a contrast agent.

Kim *et al*. [235] synthesized ferrofluids for MRI contrast agents by coating them with oleic acid as a surfactant and then dispersed them in the chitosan, which is a suitable carrier for bioapplications. They compared the MRI images of the ferrofluids with the images of Resovists® (a commercially available contrast agent for MRI). Their study showed that the ferrofluids exhibited enhancement of the MRI contrasts

comparable to Resovist® *in vitro*.

However, MRIs are not convenient for *in situ* monitoring, thus a sensitive and simple technique for *in situ* monitoring of the NPs in living cells is desirable. Compared to a conventional organic fluorescence probes, advantages of the nanometer-sized fluorescence probes mainly include their higher photostability and stronger fluorescence. The main problem in cell imaging using the fluorescent nanoprobes is that the fluorescence signal is easily affected by the background noises caused by the cells, matrix and the non-specific scattering lights. The high signal to noise (S/N) ratio is difficult to be obtained. Recently, Wu *et al*. [236] prepared multifunctional nanoparticles which possess magnetic, long-life fluorescence and bio-affinity properties. They used the nanoparticle-labeled for time-resolved fluorescence cell imaging of Hela cells. They found that the time-resolved fluorescence imaging technique is favourably useful to eliminate the background noises caused by cells and matrix. These properties of the silica-based magnetic-fluorescent nanoparticles lead to application advantages in biological labeling and detection, cell separation with drug and gene delivery over the conventional probes.

Hyperthermia

Placing superparamagnetic iron oxide in AC magnetic fields randomly flips the magnetization direction between parallel and antiparallel orientations, allowing the transfer of magnetic energy to the particles in the form of heat, a property that can be used *in* v*ivo* to increase the temperature of tumor tissues to destroy the pathological cells by hyperthermia. Tumor cells are more sensitive to a temperature increase than healthy ones [237,238].

In past studies, magnetite cationic liposomal nanoparticles [239,240] and dextran-coated magnetite [241] have been shown to effectively increase the temperature of tumor cells for hyperthermia treatment in cell irradiation. This has been proposed to be one of the key approaches to successful cancer therapy in the future [242].

Catalysis Applications

The facile recovery and reuse of homogeneous catalysts *via* covalent tethering to a heterogeneous support while maintaining high catalytic activity has long been a goal in catalysis research [243]. Thus, during the past two decades, a great deal of attention has been paid to developing methods for heterogenizing homogeneous catalysts in order to combine the advantages of both homogeneous and heterogeneous catalysis [244,245]. Among these methods, the binding of catalysts to organic polymer solids [246,247] or inorganic solids [248] has become widely used. Although the heterogenized catalysts can be recycled and easily separated from the reaction mixtures, they are significantly less reactive and selective than their homogeneous counterparts. For this reason, there is a need to find new methods and strategies in order to overcome these limitations. In recent years, catalysts supported on MNPs have been extensively used to improve limitation of heterogeneous catalysis. Magnetically driven separations make the recovery of catalysts in a liquid-phase reaction much easier than using cross flow filtration and centrifugation, especially when the catalysts are in the sub-micrometer size range. Such small and magnetically separable catalysts could combine the advantages of high dispersion and reactivity with easy separation. In terms of recycling expensive catalyst or ligands, immobilization of these active species on MNPs leads to the easy separation of catalysts in a quasi-homogeneous system [24].

The various types of transition metal-catalyzed reactions using catalytic sites grafted onto MNPs that have emerged recently include carbon-carbon cross-coupling reactions [249,250], hydroformylation [251], hydrogenation [192,252] and polymerization [253] reactions. Other reports on MNP-supported catalysts include enzymes for carboxylate resolution [254], amino acids for ester hydrolysis [255] and organic amine catalysts promoting Knoevenagel and related reactions [256].

Lin *et al*. [192] recently synthesized a novel magnetically recoverable heterogenized chiral catalyst through immobilizing a ruthenium(II) complex, [Ru (binap-PO_3H_2)-(dpen)Cl_2] magnetite nanoparticles through the phosphonate group. The heterogenized catalysts can be readily recycled by magnetic decantation and used for asymmetric hydrogenation aromatic ketones for up to 14 times without loss of activity and enantioselectivity. Dálaigh *et al*. [193] immobilized dimethylaminopyridine (DMAP) analogue on silica coated MNPs to use as a robust heterogeneous nucleophilic catalyst of unprecedented activity and recyclability. In their study, the ease of recovery, combined with the intrinsic stability of both

the organic and nanoparticle catalyst components, allows the catalyst to be recycled over 30 times in a number of transformations without any discernible loss in activity.

Studies to further explore the potential of this powerful immobilization strategy for the preparation of other heterogeneous catalysts of high synthetic utility based on MNPs are underway.

Environmental Applications

Iron NPs technology is considered to be among the first generation of nanoscale environmental technologies [257,258]. This technology could provide cost-effective solutions to some of the most challenging environmental cleanup problems [259]. Over the past decade, permeable reactive barriers have been developed, as alternatives for the conventional *pump-and-treat* technology, used to treat groundwater contaminated by different pollutants [260]. In these barriers, nZVI can be used as a reactive material due to its great ability to reduce and stabilise different types of compounds, when zero-valent iron is synthesised on the nanoscale, the uptake capacity increases largely due to the enlargement in surface area and the density of reactive sites [261]. An equally important property of nanoscale iron particles is their enormous flexibility for *in situ* applications. Modified iron nanoparticles, such as catalysed and supported nanoparticles, have been synthesised to further enhance their speed and efficiency of remediation [260]. In spite of some still unresolved uncertainties associated with the application of iron nanoparticles, this material is being accepted as a versatile tool for the remediation of different types of contaminants in groundwater, soil and air on both the experimental and field scales [262]. Beside of lots of advantages of nZVI, a major drawback is its sensitivity to oxidation in air and aqueous solutions. In recent years other MNPs have been investigated for the removal of organic and inorganic pollutants.

Organic Pollutants

Up to date, in literature there are a few articles about the removal of high concentrations of organic compounds which are mostly related to the removal of dyes. Table 1 shows different modified MNPs which have been used for this purpose. The tabulated results show that the MNPs have a high capacity in removal of high concentrations of organic compounds [263-267]. Dyes are present in the wastewater streams of many industrial sectors such as, dyeing, textile factories, tanneries, and in the paint industry. Therefore, the replacing of MNPs with expensive or low efficient adsorbent for treatment of textile effluent can be a good platform which need to more detailed investigations.

Also, Li *et al*. [268] evaluated NANOCAT® Superfine Fe_2O_3 NPs both as a catalyst and as an oxidant for the removal of carbon monoxide *via* oxidation. They found that the NPs are much more effective as carbon monoxide catalysts than the non-nano oxide powder. In the absence of oxygen, a Fe_2O_3 nanoparticle oxidizes carbon monoxide directly as an oxidant.

Inorganic Pollutants

A very important aspect in metal toxin removal is the preparation of functionalized sorbents for affinity or selective removal of hazardous metal ions from complicated matrices [193,197,269-278]. Table 2 shows some of recently published articles of literature which have used MNPs as sorbents for the removal of metal ions. For example, Wang *et al*. [269] recently reported the use of bisphosphate-modified MNPs to remove radioactive metal toxins (*e.g.*, UO_2^{2+}) with a high efficiency, from blood. In their study, they found that the designed MNPs can remove 69% of the initial UO_2^{2+} from blood containing 100 ppm of the ion. They also suggested that these functionalized, biocompatible MNPs can act as useful and effective agents for selective and rapid removal of radioactive metal toxins *in vivo*. Very recently, Lee *et al*. [270] readily prepared BODIPY-functionalized magnetic silica NPs for a high affinity and high selectivity removal of Pb^{2+} from water and human blood. Their findings may lead to the development of a new type of tailor made biocompatible system, built by immobilizing the appropriate fluorescence receptors onto the surface of novel magnetic nanomaterials for the detection, recovery, and removal of other heavy metal toxins from the human body. Thus, MNPs show a high capacity and efficiency for the removal of different metal ions due to their high surface area in respect to micron-sized sorbents, (Table 2). These findings can be used to design an appropriate adsorption treatment plant for removal and recovery of metal ions from wastewaters.

Analytical Applications

Fluorescence techniques. Due to small size of magnetic luminescent NPs, that offers a larger surface area-to-volume ratio than currently used microbeads, which result in a good reaction homogeneity and faster reaction kinetics. Thus, the preparation of magnetic fluorescent particles, such as polystyrene magnetic beads with entrapped organic dyes/quantum dots (QDs) [279,280] or shells of QDs [281], iron oxide particles coated with dye-doped silica shells [282], and silica NPs embedded with iron oxide and QDs [283,284]. However, their application is limited, mostly to biological applications such as cellular imaging. Only a few papers have reported the use of dual-functional NPs for multiplexed quantitative bioanalysis [285,286].

Nichkova *et al*. [287] reported a new detection format for multiplexed analysis based on the use of magnetic luminescent Co:Nd:Fe_2O_3/Eu:Gd_2O_3 NPs (MLNPs). The steps of multiplexed fluoroimmunoassay with MLNPs are shown in Fig. 8. The magnetic properties of the MLNPs allowed their manipulation by an external magnetic field without the need of centrifugation or filtration. Their optical characteristics (sharp emission, photostability, long lifetime) facilitated the implementation of an internal calibration in the detection system. This introduced a unique internal quality control and an easy quantifications in the multiplexed immunoanalysis. This method developed and enables a direct, simple, and quantitative multiplex protein analysis using conventional organic dyes and can be applied for disease diagnostics and detection of biological threats. Furthermore, they found that MLNPs with different emission wavelengths can be easily obtained by controlled doping of different lanthanide ions (*e.g.*, Eu and Tb) into the host material, making them very attractive as a ‘‘bar-coding’’ tool. The ability to use the MLNPs for both separation and detection makes them valuable tools for a wide range of biotechnology applications, such as carriers with magnetic orientation and fluorescence tracers for potent drug targeting.

For the first time Wang *et al*. [269] immobilized a fluorescence receptors on MNPs for the removal of a metal toxin from blood. Then Lee *et al*. [270] reported

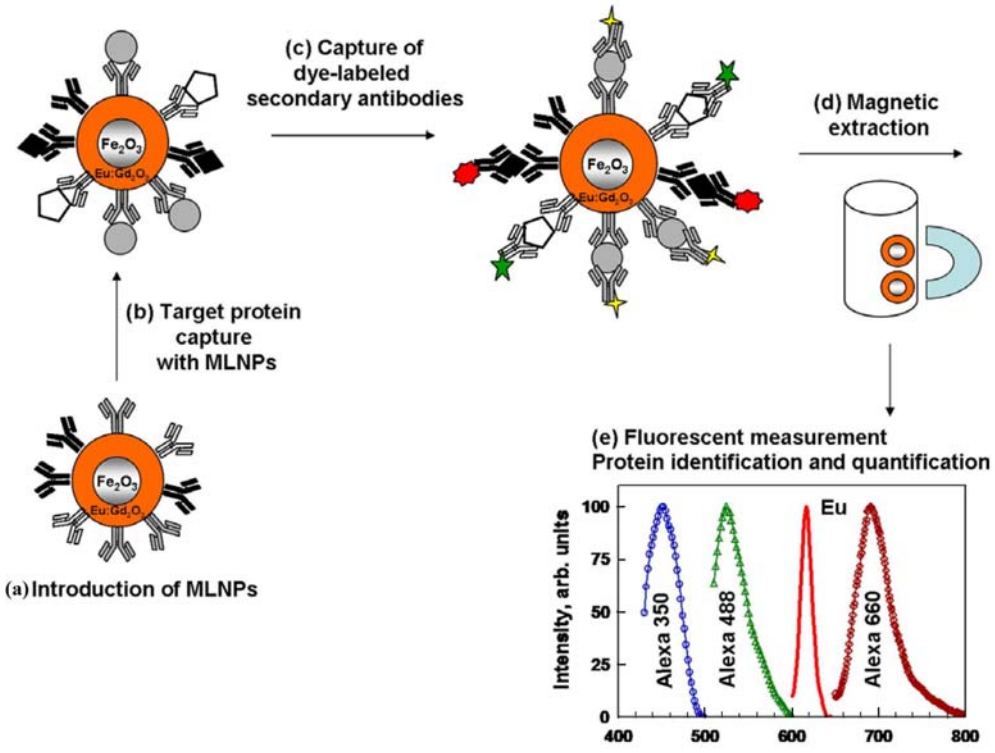

Fig. 8. Multiplexed fluoroimmunoassay with magnetic luminescent nanoparticles (MLNPs) [287].

immobilization of 4,4-difluoro-4-bora-3a, 4adiaza-s-indacene (BODIPY) on MNPs for the removal of Pb^{2+} from blood. In their study, BODIPY was selected as a signal-transducing unit because it absorbs and emits in the visible region with high excitation coefficients, high fluorescent quantum yields, and high photostability [288]. Also, their results showed that fluorescence intensities of Pb^{2+}-BODIPY/Ni@SiO_2 are unchanged in the presence of Li^+, Na^+, Mg^{2+}, K^+, Ca^{2+}, Cu^{2+}, Zn^{2+}, Ag^+, Cd^{2+} and Hg^{2+}, indicating that BODIPY/Ni@SiO_2 is very promising as a selective adsorbent for the separation of Pb^{2+} *in vivo*.

These techniques may lead to the development of a new type of tailor made biocompatible system built by immobilizing the appropriate fluorescence receptors onto the surface of novel magnetic nanomaterials for the detection, recovery, and removal of other compounds from the human body and environment.

Samples Preparation Methods

Solid phase extraction (SPE). SPE is a routine extraction method for determining trace level contaminants in environmental samples. Recently, nanometer-sized particles (nanoparticles, NPs) have gained rapid and substantial progress, and have significantly an impact on sample extraction [289-300].

Nanomaterials can offer several advantages over traditional SPE sorbents such as having very high surface areas and a short diffusion route, which result in their high extraction capacity, rapid extraction dynamics and high extraction efficiencies [301,302]. Another advantage of NPs is that NPs' surface functionality can be easily modified to achieve selective sample extraction [303,304]. However, the use of nanomaterials with a sub-100 nm size range has some inherent limitations, especially when applied in the adsorption and separation of contaminations from large volumes of environment samples. When column dynamic extraction mode is used, the nanosized particles packed SPE column exhibits a high backpressure, making it very difficult to adopt high flow rates; when the static batch mode is used, the nanosized SPE adsorbents often lead to a very low filtration rate.

Among different kinds of NPs, magnetic NPs, mainly Fe_3O_4 NPs, appears as an interesting advanced composite material. It has received increasing attention in the past decades due to its unique physical and chemical properties which can easily couple with magnetic carrier technology (MCT) which was first reported by Robinson in 1973 [305]. By applying this technology, MNPs with adsorbed samples can be easily collected by using an external magnetic field placed outside of the extraction container without additional centrifugation or filtration of the sample, which makes sampling and collection easier and faster. Moreover, the MNPs may be reused or recycled.

The majority of the preliminary works reported has been focused on the extraction of big biomolecules such as peptides, proteins and DNAs, isolation of small molecules including salicylamide, mefenamic acid, ketoprofen, flufenamic acid and triazines by using magnetic NPs [306]. In the reported works, retained analytes on NPs were quantified by using MALDI-MS this is not an ideal technique for quantitative analysis in comparison with HPLC-ESI-MS. In fact, in all of the developed NP-based sample extraction procedures [389-300] except one [389] the authors have applied MALDI-MS for final analysis. This was very likely because there is no need to recover the analytes retained on NPs using eluents MALDI-MS analysis. Because elution of the analytes bound to NPs can be very difficult, if not impossible to recover.

Recently, utility and performance of MNPs as SPE adsorbents for preconcentration and quantitative determinations at trace level of organic and inorganic molecules have been investigated by some research groups and the results are tabulated in Table 3. Based on the reported results the retained analysts have eluted from the surface of MNPs with suitable eluent before determination of them by using conventional detection systems. Also it can be concluded that, up to date, the SPE sorbents obtained via coating of the magnetic sorbents with ionic surfactants through electrostatic attraction and/or further functionalization of magnetic sorbents with suitable functional groups with covalent conjugations.

SPE method based on mixed hemimicelles (hemimicelles and admicelles) (MHSPE) is a new method which has been proposed for the preconcentration of a variety of organic compounds from aqueous matrices. In this method, the sorbents used are produced by the adsorption of ionic surfactants, such as sodium dodecyl sulphate (SDS) or

cetyltrimethylammonium bromide (CTAB) onto the surface of metal oxides. Depending on the amount of added surfactant, they can form different structures on the surface of metal oxides. Hemimicelles consist of monolayers of surfactants adsorbed head down on an oppositely charged mineral oxide surface. Admicelles are surfactant bilayers formed from hemimicelles, under the addition of more surfactant, by interaction of surfactant hydrocarbon chains. The use of mixed hemimicelles assemblies in SPE has a number of advantages, such as the adsorption is driven by hydrophobic interactions and electrostatic attraction, high extraction yield, easy elution of analytes and high breakthrough volume. Furthermore, the sorbents of this MHSPE technique are easy to regenerate [306-309]. However, the applications of hemimicelles and admicelles based SPE reported in literatures were mainly based on ionic surfactants adsorbed onto micron-size particles. Since the micron-size particles have comparatively small surface areas, they may lead to a relatively low extraction efficiency and concentration factor. The advantages of MHSPE and MNPs can combine to fabricate magnetic nanosized MHSPE adsorbents with high surface areas, high chemical stability and rapid magnetic separability. It can be assumed that its application in analytical chemistry can improve the adsorption capacity of analytes, avoid the time-consuming enrichment process of loading large volumes of samples in conventional SPE method. In the literatures, there have been a few applications that reported this technology so far [170,171]. For the first time, Zhao *et al*. [170] studied MHSPE based on CTAB-coated MNPs for the preconcentration of phenolic compounds from environmental water samples. Schematic illustration of the preparation of surfactants coated Fe_3O_4/SiO_2 NPs and its application as an SPE sorbent is shown in Fig. 9 [171]. Afterward, this method was developed by other research groups. The obtained results from literature have shown that MHSPE can be a simple and efficient methodology for preconcentration of organic and inorganic compounds from large volumes of samples.

Beside of MHSPE method, in literature there are a few works about the application of surfactant coated MNPs as sorbents for preconcentration and quantitative determination of trace amounts of compounds [310-315]. For example, Song *et al*. [311] used bilayer decanoic acid coated Fe_3O_4 NPs as an extract agent for preconcentration of triazine pesticides from large volume samples and they eluted the preconcentrated analytes using 10.0 M HCl before HPLC-ESI-MS/MS analysis. In the same method, Yamini *et al*. [312] developed application of monolayer decanoic acid coated Fe_3O_4 NPs as a sorbent for preconcentration of trace amounts of heavy metal ions in water samples. Moreover, Zargar *et al*. [313] used SDS-bounded iron oxide NPs as sorbents for preconcentration and determination of basic fuchsin (BF) in aqueous solutions. Yamini and co-workers [314] investigated application of SDS-

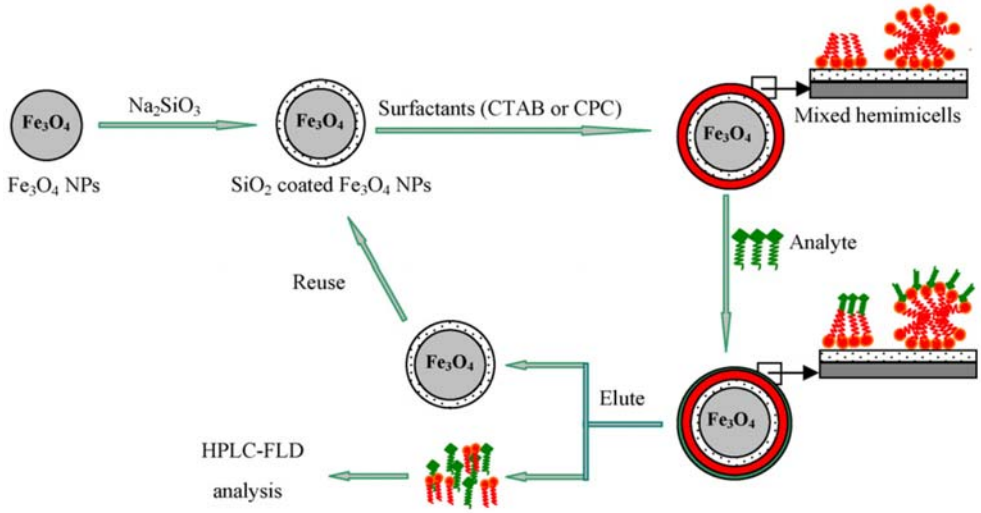

Fig. 9. Schematic illustration of the preparation of surfactants coated Fe_3O_4/SiO_2 NPs and its application for enrich analytes as SPE sorbents [171].

coated Fe_3O_4 NPs for the extraction of trace amounts of mercury from environmental samples, their procedure is based on the adsorption of analytes as mercury-Michler's Thioketone $[Hg_2(TMK)_4]^{2+}$ complex on negatively charged surfaces of the SDS-Fe_3O_4 NPs and then elution of the preconcentrated mercury from the surfaces of SDS-Fe_3O_4 NPs prior to its determination by flow injection inductively coupled plasma-optical emission spectrometry. Due to magnetically assisted-separation of the sorbent, the applied method on large volumes of water samples (1000 ml) resulted in a high enhancement factor with a low detection limit.

More recently, by covalent conjugation of different functional groups on the surface of MNPs various SPE, sorbents have been prepared for selective extraction of the organic and inorganic compounds. Up to date, functionalized MNPs with octadecyl (C_{18}) [316,317], γ-mercaptopropyl-trimethoxysilane (γ-MPTMS) [3318,319] and bismuthiol [320] have been used for quantitative determination of trace amounts of inorganic and organic compounds. The reported SPE methods based on MNPs (Table 3) show that their sensitivity is very good. Also, by using MNPs sorbents, high preconcentration factors and low detection limits in a shorter time can be achieved due to their large surface area, rapid dynamics of extraction and the high extraction efficiencies of the MNPs. Compared to traditional SPE methods with micron-sized sorbent materials, these types of SPE methods with nano-sized sorbent materials have advantages, such as (a) being low time-consuming due to magnetically-assisted separation of the adsorbent, which can meet the needs of rapid analysis, (b) the MNP adsorbents have higher surface areas; therefore, satisfactory results can be achieved by using less amounts of the NPs adsorbents and (c) The MNP sorbents can be easily synthesized in a laboratory.

Due to advantages of the magnetic sorbents, studies to further explore the potential applications of these sorbents for affinity and/or selective extraction of organic and inorganic compounds are underway. In other words, a main trend in this field is the preparation of sorbents with specific functional groups for selective extraction.

Molecular Imprinting Polymer (MIP)

MIP technique is an attractive method for the generation of polymer-based molecular recognition of elements tailor-made for a given target, or group of target molecules [321,322].

However, they suffer from some drawbacks in certain applications, such as the heterogeneous distribution of the binding sites, low binding capacity and selectivity, poor site accessibility and slow binding kinetics. The development of molecular imprinting nanotechniques will provide a potential solution to overcome these problems [323-328]. Nanosized molecular imprinted materials (MIP nanoparticles [323,324], MIP nanocapsule [325], MIP nanowire [326,327], MIP nanotube [328]) having a small dimension with a high surface-to-volume ratio are expected to improve the removal of template molecules, the binding capacity as well as the fast binding kinetics over normal imprinting materials.

Although, incorporating magnetic nanoprticles and MIP have been introduced previously by some research groups [329-331] the prepared magnetic composites were in micron or sub-micron dimension. More recently, Wang *et al*. [332] developed a new methodology for preparing MNPs attached functional moieties of specific recognition with tailor-made properties through a molecular imprinting technique. Multistep synthesis of estrone-imprinted MNPs and Synthesis of template-silica monomer complex are shown in Fig. 10. They explored synthesis of estrone-imprinted polymer coated Fe_3O_4 MNPs that exhibit a much higher specific recognition and saturation magnetization. The results showed that in comparison with traditional MIPs nanoparticles, the molecular imprinted magnetic hybrid display several advantages: (a) the superparamagnetic iron oxide core enables the particles to replace the centrifugation step with a magnetic separation, and facilitates the application of magnetic MIP in immunoassay and magnetically stabilized-fluidised-bed separation; (b) The semi-covalent imprinting can be looked upon as a hybrid approach in which the imprinting is covalent, but the rebinding is noncovalent in nature; (c) There are no randomly distributed functional groups and the binding sites are more uniform in nature [333]; (d) The template removal by hydrolysis leaves the binding sites in the silica shell during the imprinting step, and the template molecules can reach the imprinting sites easily and quickly during the rebinding step.

This work can provide a platform to prepare molecularly imprinted polymer modified MNPs with high affinity, selectivity and capacity to nearly any target molecules. Also, such nano MIP can be one of the most promising candidates

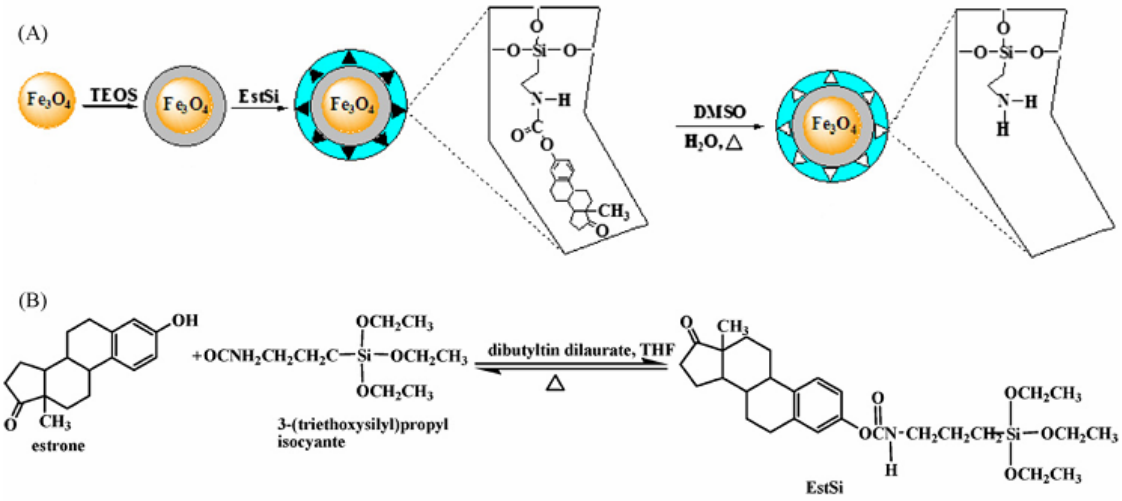

Fig. 10. (A) Multistep synthesis of estrone-imprinted MNPs. (B) Synthesis of template-silica monomer complex (EstSi) [332].

for various applications, including chemical and biochemical separation, cell sorting, recognition elements in biosensors and drug delivery.

SUMMARY AND OUTLOOKS

The synthesis of MNPs, covering a wide range of compositions and tuneable sizes, has made substantial progress especially over the past decade. Different kinds of monodisperse spherical nanocrystals with controllable particle sizes and compositions have been synthesized by a wide range of chemical synthetic procedures. However, from a synthetic point of view, there are several interesting research areas worth pursuing. First, synthesis of high-quality MNPs in a controlled and reproducible manner resulting in a homodisperse population of magnetic grains of controllable size. Second, detailed understanding of the synthetic mechanisms of nucleation and growth during particle formation which is still a challenge. Third, it is equally important to develop methods based on aqueous systems that are environmentally friendly in order to omit the large amounts of toxic organic solvents, precursors and surfactants. Fourth, the coupling of hydrothermal and thermal decomposition methods as techniques for high quality synthesis of MNPs with microwave and ultrasonic techniques in order to develope convenient, fast and single step processes. Sixth, synthesis of biocompatible MNPs (chemically stable, uniform in size and well dispersed in liquid media) in a single step with effective surface coatings that provides optimum performance *in vitro* and *in vivo* biological applications. Seventh, development of a large-scale particle production processes.

An unavoidable problem associated with nanoparticles is their intrinsic instability over long periods of time. Among the coating materials reviewed, silica's have a lot of benefits but are not stable under basic conditions, on the other hand, carbon-coated MNPs are remarkably stable under harsh conditions (high temperatures and under acidic and basic conditions). But, generation of a carbon coating on individual dispersed nanoparticles and the control of the shell thickness still remain an unresolved problem. Therefore, there is still a need to explore novel synthetic methods to ensure the stability of MNPs at harsh conditions with controllable shell thickness.

In recent years, a trend in the synthesis of MNPs and preparation of monodisperse hollow nanoprticles was achieved [149,334-336]. Hollow NPs with controlled interior voids and shell thicknesses are an important class of nanoporous materials. With large surface areas and low material density, these nanoparticles could serve as ideal building blocks for the fabrication of lightweight structural materials and for catalysis, nanoelectronics and drug-delivery applications. Synthesis of these types of nanoparticles should be studied for detailed understanding.

The surface functionalization and modification of MNPs

to introduce additional functionality will gain more and more attention in coming years. Complex, multifunctional magnetic nanoparticle systems with designed active sites, including ligands, fluorophores, enzymes, catalysts, drugs and other species, seem to be promising for a variety of applications. In this area, functionalization for affinity or selective targeting can be an active research field.

Another aspect is removal of MNPs from the environment. The rapidly increasing production of engineered nanoparticles has created a demand for particle removal from industrial and communal wastewater streams. Efficient removal is particularly important in view of increasing long-term persistence and evidence for considerable ecotoxicity of specific nanoparticles [337].

Finally, to improve our understanding of such systems and their applications, a collaborative multidiscipline effort is anticipated.

ACKNOWLEDGEMENTS

Financial support from Tarbiat Modares University is greatfully acknowledged.

REFERENCES

[1] R.C. O'Handley, Modern Magnetic Materials: Principles and Applications, Wiley, New York, 2000.
[2] N. Spaldin, Magnetic Materials: Fundamentals and Device Applications, Cambridge University Press, Cambridge, UK, 2003.
[3] R.M. Cornell, U. Schwertmann, The Iron Oxide: Structure, Properties, Reactions, Occurrences and Uses, Wiley-VCH, Weinheim, Germany, 2003.
[4] K.J. Klabunde (Ed.), Nanoscale Materials in Chemistry, Wiley-Interscience, New York, 2001.
[5] G. Schmid (Ed.), Nanoparticles, Wiley-VCH, Weinheim, 2004.
[6] A.P. Alivisatos, Science 271 (1996) 933.
[7] A.L. Rogach, D.V. Talapin, E.V. Shevchenko, A. Kornowski, M. Haase, H. Weller, Adv. Funct. Mater. 12 (2002) 653.
[8] T. Hyeon, Chem. Commun. 8 (2003) 927.
[9] M.G. Bawendi, M.L. Steigerwald, L.E. Brus, Annu. Rev. Phys. Chem. 41 (1990) 477.
[10] M.A. El-Sayed, Acc. Chem. Res. 34 (2001) 257.
[11] Z. Xu, F.-S. Xiao, S.K. Purnell, O. Alexeev, S. Kawi, S.E. Deutsch, B.C. Gates, Nature 372 (1994) 346.
[12] L. Spanhel, M. Haase, H. Weller, A. Henglein, J. Am. Chem. Soc. 109 (1987) 5649.
[13] M.L. Steigerwald, L.E. Brus, Annu. Rev. Mater. Sci. 19 (1989) 471.
[14] M.L. Steigerwald, L.E. Brus, Acc. Chem. Res. 23 (1990) 183.
[15] A.N. Goldstein, C.M. Echer, A.P. Alivisatos, Science 256 (1992) 1425.
[16] M.J. Bruchez, M. Moronne, P. Gin, S. Weiss, A.P. Alivisatos, Science 281 (1998) 2013.
[17] W.C.W. Chan, S. Nie, Science 281 (1998) 2016.
[18] I.L. Medintz, H.T. Uyeda, E.R. Goldman, H. Mattoussi, Nat. Mater. 4 (2005) 435.
[19] X. Michalet, F.F. Pinaud, L.A. Bentolila, J.M. Tsay, S. Doose, J.J. Li, G. Sundaresan, A.M. Wu, S.S. Gambhir, S. Weiss Science 307 (2005) 538.
[20] J.M. Klostranec, W.C.W. Chan, Adv. Mater. 18 (2006) 1953.
[21] Y. Yin, A.P. Alivisatos, Nature 437 (2005) 664.
[22] J. Park, J. Joo, S.G. Kwon, Y. Jang, T. Hyeon, Angew. Chem., Int. Ed. 46 (2007) 4630.
[23] U. Jeong, X. Teng, Y. Wang, H. Yang, Y. Xia, Adv. Mater. 19 (2007) 33.
[24] A.-H. Lu, E.L. Salabas, F. Schüth, Angew. Chem., Int. Ed. 46 (2007) 1222.
[25] D.S. Mathew, R.-S. Juang, Chem. Eng. J. 129 (2007) 51.
[26] S. Laurent, D. Forge, M. Port, A. Roch, C. Robic, L.V. Elst, R.N. Muller, Chem. Rev. 108 (2008) 2064.
[27] W. Wu, Q. He, C. Jiang, Nanoscale Res. Lett. 3 (2008) 397.
[28] A.S. Teja, P.-Y. Koh, Progress in Crystal Growth and Characterization of Materials 55 (2009) 22.
[29] C. Chen, Magnetism and Metallurgy of Soft Magnetic Materials, Dover Publications, Inc., New York, 1986.
[30] C.M. Sorensen, in: K.J. Klabunde (Ed.), Nanoscale Materials in Chemistry, Wiley, New York, 2001.
[31] A.H. Morrish, The Physical Principles of Magnetism, Wiley, New York, 1965.

[32] E.C. Stoner, E.P. Wohlfarth, A Mechanism of Magnetic Hysteresis in Heterogeneous Alloys, Philos. Trans. R. Soc. A 240 (1948) 599.
[33] S.-J. Park, S. Kim, S. Lee, Z. Khim, K. Char, T. Hyeon, J. Am. Chem. Soc. 122 (2000) 8581.
[34] V.F. Puntes, K.M. Krishan, A.P. Alivisatos, Science 291 (2001) 2115.
[35] X. Sun, A. Gutierrez, M.J. Yacaman, X. Dong, S. Jin, Mater. Sci. Eng. A 286 (2000) 157.
[36] S. Neveu, A. Bee, M. Robineau, D. Talbot, J. Colloid Interface Sci. 255 (2002) 293.
[37] F. Grasset, N. Labhsetwar, D. Li, D.C. Park, N. Saito, H. Haneda, O. Cador, T. Roisnel, S. Mornet, E. Duguet, J. Portier, J. Etourneau, Langmuir 18 (2002) 8209.
[38] S. Sun, H. Zeng, J. Am. Chem. Soc. 124 (2002) 8204.
[39] J. Hu, I.M.C. Lo, G. Chen, Sep. Purif. Technol. 56 (2007) 249.
[40] J. Park, K. An, Y. Hwang, J.-G. Park, H.-J. Noh, J.-Y. Kim, J.-H. Park, N.-M. Hwang, T. Hyeon, Nat. Mater. 3 (2004) 891.
[41] S. Sun, C.B. Murray, D. Weller, L. Folks, A. Moser, Science 287 (2000) 1989.
[42] E.V. Shevchenko, D.V. Talapin, A.L. Rogach, A. Kornowski, M. Haase, H. Weller, J. Am. Chem. Soc. 124 (2002) 11480.
[43] V. LaMer, R. Dinegar, J. Am. Chem. Soc. 72 (1950) 4847.
[44] H. Iida, K. Takayanagi, T. Nakanishi, T. Osaka, J. Colloid Interface Sci. 314 (2007) 274.
[45] L. Babes, B. Denizot, G. Tanguy, J.J. Le Jeune, P.J. Jallet, Colloid Interface Sci. 212 (1999) 474.
[46] E. Tronc, P. Belleville, J.-P. Jolivet, J. Livage, Langmuir 8 (1992) 313.
[47] R.F. Ziolo, E.P. Giannelis, B.A. Weinstein, M.P. O'Horo, B.N. Ganguly, V. Mehrotra, M.W. Russell, D.R. Huffman, Science 257 (1992) 219.
[48] L. Zhang, G.C. Papaefthymiou, J.Y.J. Ying, Appl. Phys. 81 (1997) 6892.
[49] L. Shen, P.E. Laibinis, T.A. Hatton, Langmuir 15 (1999) 447.
[50] R.Y. Hong, J.H. Li, H.Z. Li, J. Ding, Y. Zheng, D.G. Wei, J. Magn. Magn. Mater. 320 (2008) 1605.
[51] C.Q. Hu, Z.H. Gao, X.R. Yang, Chem. Phys. Lett. 429 (2006) 513.
[52] X. Qui, Chin. J. Chem. 18 (2000) 834.
[53] R. Massart, V. Cabuil, J. Chim. Phys. 84 (1987) 7.
[54] A.K. Gupta, S. Wells, IEEE Trans. Nanobiosci. 3 (2004) 66.
[55] D.K. Kim, Y. Zhang, W. Voit, K.V. Rao, M. Muhammed, J. Magn. Magn. Mater. 30 (2001) 225.
[56] Z.L. Liu, H.B. Wang, Q.H. Lu, G.H. Du, L. Peng, Y.Q. Du, S.M. Zhang, K.L. Yao, J. Magn. Magn. Mater. 283 (2004) 258.
[57] J.A. Lopez Perez, M.A. Lopez Quintela, J. Mira, J. Rivas, S.W. Charles, J. Phys. Chem. B 101 (1997) 8045.
[58] J.A. Lopez Perez, M.A. López-Quintela, J. Mira, J. Rivas, IEEE Trans. Magn. 33 (1997) 4359.
[59] P.A. Dresco, V.S. Zaitsev, R.J. Gambino, B. Chu, Langmuir 15 (1999) 1945.
[60] K.M. Lee, C.M. Sorensen, K.J. Klabunde, G.C. Hadjipanayis, IEEE Trans. Magn. 28 (1992) 3180.
[61] C. Liu, B. Zou, A.J. Rondinone, Z.J. Zhang, J. Phys. Chem. B 104 (2000) 1141.
[62] S. Santra, R. Tapec, N. Theodoropoulou, J. Dobson, A. Hebard, W. Tan, Langmuir 17 (2001) 2900.
[63] J. Vidal-Vidal, J. Rivas, M.A. López-Quintela, Colloid Surf. A 288 (2006) 44.
[64] S.G. Kwon, Y. Piao, J. Park, S. Angappane, Y. Jo, N.-M. Hwang, J.-G. Park, T. Hyeon, J. Am. Chem. Soc. 129 (2007) 12571.
[65] Y. Chen, D.-L. Peng, D. Lin, X. Luo, Nanotechnology 18 (2007) 505703.
[66] F. Davar, Z. Fereshteh, M. Salavati-Niasari, J. Alloys Compd. 476 (2009) 797.
[67] T. Hyeon, S.S. Lee, J. Park, Y. Chung, H.B. Na, J. Am. Chem. Soc. 123 (2001) 12798.
[68] S. Sun, H. Zeng, D.B. Robinson, S. Raoux, P.M. Rice, S.X. Wang, G. Li, J. Am. Chem. Soc. 126 (2004) 273.
[69] Y. Chen, D.-L. Peng, D. Lin, X. Luo, Nanotechnology 18 (2007) 505703.
[70] K. Butter, K. Kassapidou, G.J. Vroege, A.P. Philipse, J. Colloid Interface Sci. 287 (2005) 485.
[71] B. Mao, Z. Kang, E. Wang, S. Lian, L. Gao, C. Tian, C. Wang, Mater. Res. Bull. 41 (2006) 2226.
[72] H. Zhu, D. Yang, L. Zhu, Surf. Coat. Technol. 201 (2007) 5870.
[73] S. Giri, S. Samanta, S. Maji, S. Ganguli, A. Bhaumik, J. Magn. Magn. Mater. 285 (2005) 296.
[74] J. Wang, J. Sun, Q. Sun, Q. Chen, Mater. Res. Bull. 38

(2003) 1113.
[75] F. Gözüak, Y. Köseoğlu, A. Baykal, H. Kavas, J. Magn. Magn. Mater. 321 (2009) 2170.
[76] J. Wang, F. Ren, R. Yi, A. Yan, G. Qiu, X. Liu, J. Alloys Compd. 479 (2009) 791.
[77] A.S. Teja, L.J. Holm, in: Y.P. Sun (Ed.), Production of Magnetic Oxide Nanoparticles, Supercritical Fluid Technology in Materials Science and Engineering: Synthesis, Properties and Applications, Elsevier, 2002, pp. 327-349.
[78] Y. Hao, A.S. Teja, J. Mater. Res. 18 (2003) 415.
[79] C. Xu, A.S. Teja, J. Supercrit. Fluids 44 (2008) 85.
[80] S. Komarneni, H. Katsuki, Pure Appl. Chem. 74 (2002) 1537.
[81] V. Sreeja, P.A. Joy, Mater. Res. Bull. 42 (2007) 1570.
[82] Y. Hou S. Gao, J. Mater. Chem. 13 (2003) 1510.
[83] M. Green, P. O'Brien, Chem. Commun. (2001) 1912.
[84] Y.-P. Sun, X.-Q. Li, W.-X. Zhang, H.P. Wang, Colloid Surf. A 308 (2007) 60.
[85] Y.-P. Sun, X.-Q. Li, J. Cao, W.-X. Zhang, H.P. Wang, Adv. Colloid Interface Sci. 120 (2006) 47.
[86] T.J. Mason, J.P. Lorimal, Applied Sonochemistry, New York, Wiley, 2002.
[87] E.H. Kima, H.S. Lee, B.K. Kwak, B.-K. Kim, J. Magn. Magn. Mater. 289 (2005) 328.
[88] V.V. Namboodiri, R.S. Varma, Green Chem. 3 (2001) 146.
[89] S. Komarneni, Curr. Sci. 85 (2003) 1730.
[90] W.-W. Wang, Mater. Chem. Phys. 108 (2008) 227.
[91] W.-W. Wang, Y.-J. Zhu, M.-L. Ruan, J. Nanopart. Res. 9 (2007) 419.
[92] H.O. Pierson, Handbook of Chemical Vapor Deposition: Principles, Technology and Applications, William Andrew Inc., 1999.
[93] A. Tavakoli, M. Sohrabi, A. Kargari, Chem. Pap. 61 (2007) 151.
[94] W. Chang, G. Skandan, S.C. Danforth, B.H. Kear, H. Hahn, Nanostruct. Mater. 4 (1994) 507.
[95] C. Powell, J. Oxley, J. Blocher, Vapor Deposition, John Wiley & Sons, New York, 1966.
[96] E. Flahaut, F. Agnoli, J. Sloan, C. O'Connor, M.L.H. Green, Chem. Mater. 14 (2002) 2553.
[97] Z.H. Wang, C.J. Choi, B.K. Kim, J.C. Kim. Z.D. Zhang, Carbon 41 (2003) 1751.
[98] B.H. Liu, J. Ding, Z.Y. Zhong, Z.L. Dong, T. White, J. Y. Lin, Chem. Phys. Lett. 358 (2002) 96.
[99] V.P. Dravid, J.J. Host, M.H. Teng, B. Eillott, J.H. Hwang, D.L. Johnson, Nature 374 (1995) 602.
[100] M.H. Teng, J.J. Host, J.H. Hwang, B.R. Elliott, J.R. Weertman, T.O.J. Mason, Mater. Res. 10 (1995) 233.
[101] X. Sun, A. Gutierrez, M.J. Yacaman, X. Dong, S. Jin, Mater. Sci. Eng. A 286 (2000) 157.
[102] T. Hirano, T. Oku, K. Suganuma, Diamond Related Mater. 9 (2000) 476.
[103] M. Kuno, T. Oku, K. Suganuma, Scr. Mater. 44 (2001) 1583.
[104] T. Oku, M. Kuno, H. Kitahara, I. Narita, Int. J. Inorg. Mater. 3 (2001) 597.
[105] X. Sun, A. Gutierrez, M.J. Yacaman, X. Dong, S. Jin, Mater. Sci. Eng. A 286 (2000) 157.
[106] J. Borysiuk, A. Grabias, J. Szczytko, M. Bystrzejewski, A. Twardowski, H. Lange, Carbon 46 (2008) 1693.
[107] K.H. Ang, I. Alexandrou, N.D. Mathur, G.A.J. Amaratunga, S. Haq, Nanotechnology 15 (2004) 520.
[108] M.P. Morales, O. Bomati-Miguel, R. Perez de Alejo, J. Ruiz-Cabello, S. Veintemillas-Vendaguer, K. Ogrady, J. Magn. Magn. Mater. 266 (2003) 102.
[109] S. Veintemillas-Vendaguer, M.P. Morales, C. Serna, J. Mater. Lett. 35 (1998) 227.
[110] S. Veintemillas-Vendaguer, M.P. Morales, O. Bomati-Miguel, C. Batista, X. Zhao, P. Bonville, R. Perez de Alejo, J. Ruiz-Cabello, M. Santos, J. Tendillo-Cortijo, J. Ferreiros, J. Phys. 37 (2004) 2054.
[111] R. Alexandrescu, I. Morjan, I. Voicu, F. Dumitrache, L. Albu, I. Soare, G. Prodan, Appl. Surf. Sci. 248 (2005) 138.
[112] E. Ye, B. Liu, W.Y. Fan, Chem. Mater. 19 (2007) 3845.
[113] J.B. Park, S.H. Jeong, M.S. Jeong, J.Y. Kim, B.K. Cho, Carbon 46 (2008) 1369.
[114] C.N. He, X.W. Du, J. Ding, C.S. Shi, J.J. Li, N.Q. Zhao, Carbon 44 (2006) 2330.
[115] J. Gavillet, A. Loiseau, C. Journet, F. Willaime, F. Ducastelle, J.C. Charlier, Phys. Rev. Lett. 87 (2001) 2755041.
[116] H. Tokoro, S. Fujiia, T. Oku, J. Mater. Chem. 14 (2004) 253.
[117] E.P. Yelsukov, A.I. Ul'yanov, A.V. Zagainov, N.B. Arsent'yeva, J. Magn. Magn. Mater. 258-259 (2003) 513.
[118] M.A. Zalich, V.V. Baranauskas, J.S. Riffle, M.

Saunders, T.G. Pierre, St. Chem. Mater.18 (2006) 2648.
[119] M. Bystrzejewski, A. Huczko, H. Lange, S. Cudziło, W. Kicínski, Diamond Relat. Mater. 16 (2007) 225.
[120] K.S. Martirosyan, L. Chang, J. Rantschler, S. Khizroev, D. Luss, D. Litvinov, IEEE Trans. Magn. 43 (2007) 157.
[121] C.F. Wang, J.N. Wang, Z.M. Sheng, J. Phys. Chem. C 111 (2007) 6303.
[122] H. Tokoro, S. Fujiia, T. Oku, J. Mater. Chem. 14 (2004) 253.
[123] R.M. Cornell, U. Schertmann, Iron Oxides in the Laboratory: Preparation and Characterization, VCH Publishers, Weinheim, Germany, 1991.
[124] S. Palmacci, L. Josephson, E.V. Groman, U.S. Patent 5, 262,176, 1995; Chem. Abstr. 1996, 122, 309897.
[125] U. Hafeli, W. Schütt, J. Teller, M. Zbrorowski, Scientific and Clinical Applications of Magnetic Carriers, Plenum Press, New York, 1997.
[126] R. Arshady, Radiolabeled and Magnetic Particles in Medicine and Biology, Vol. 3, Critrus Books, London, UK, 2001.
[127] L.N. Okassa, H. Marchais, L. Douziech-Eyrolles, S. Cohen-Jonathan, M. Souce, P. Dubois, I. Chourpa, Int. J. Pharm. 302 (2005) 187.
[128] L. Shen, P.E. Laibinis, T.A. Hatton, Langmuir 15 (1999) 447.
[129] M.H. Sousa, F.A. Tourinho, J. Depeyrot, G.J. da Silva, M.C.F.L. Lara, J. Phys. Chem. B 105 (2001) 1168.
[130] S. Sun, C.B. Murray, J. Appl. Phys. 85 (1999) 4325.
[131] Y. Lu, X. Lu, B.T. Mayers, T. Herricks, Y. Xia, J. Solid State Chem. 181 (2008) 1530.
[132] G. Carrot, D. Rutot-Houze, A. Pottier, P. Degée, J. Hilborn, P. Dubois, Macromolecules 35 (2002) 8400.
[133] A. El Harrak, G. Carrot, J. Oberdisse, C. Eychenne-Baron, F. Boué, Macromolecules 37 (2004) 6376.
[134] J. Pyun, J. Shijun, T. Kowalewski, G.D. Patterson, K. Matyjaszewski, Macromolecules 36 (2003) 5094.
[135] J.H. Fendler, Chem. Mater. 8 (1996) 1616.
[136] L.A. Harris, J.D. Goff, A.Y. Carmichael, J.S. Riffle, J.J. Harburn, T.G.S. Pierre, M. Saunders, Chem. Mater. 15 (2003) 1367.
[137] Y. Zhang, N. Köhler, M. Zhang, Biomaterials 23 (2002) 1553.
[138] M.D. Butterworth, L. Illum, S.S. Davis, Colloids Surf., A 179 (2001) 93.
[139] O. Prucker, J. Rühe, Macromolecules 31 (1998) 592.
[140] R. Jordan, N. West, A. Ulman, Y.M. Chou, O. Nuyken, Macromolecules 34 (2001) 5361.
[141] C. Yee, M. Scotti, A. Ulman, H. White, M. Rafailovich, J. Sokolov, Langmuir 15 (1999) 4314.
[142] M. Weck, J.J. Jackiw, R.R. Rossi, P.S. Weiss, R.H. Grubbs, J. Am. Chem. Soc. 121 (1999) 4088.
[143] J. Lahann, R. Langer, Macromol. Rapid Commun. 22 (2001) 968.
[144] M. Husemann, D. Mecerreyes, C.J. Hawker, L.J. Hedrick, R. Shah, N.L. Abbott, Angew. Chem., Int. Ed. 38 (1999) 647.
[145] A.M. Schmidt, Macromol. Rapid Commun. 26 (2005) 93.
[146] D. Farrell, S.A. Majetich, J.P. Wilcoxon, J. Phys. Chem. B 107 (2003) 11022.
[147] H. Bönnemann, W. Brijoux, R. Brinkmann, N. Matoussevitch, N. Waldoefner, N. Palina, H. Modrow, Inorg. Chim. Acta 350 (2003) 617.
[148] Y.-P. Sun, X.-Q. Li, J. Cao, W.-X. Zhang, H.P. Wang, Adv. Colloid Interface Sci. 120 (2006) 47.
[149] S. Peng, S. Sun, Angew. Chem. Int. Ed. 46 (2007) 4155.
[150] C.-T. Chen, Y.-C. Chen, Anal. Chem. 77 (2005) 5912.
[151] C.-Y. Lo, W.-Y. Chen, C.-T. Chen, Y.-C. Chen, J. Proteome Res. 6 (2007) 887.
[152] C.-T. Chen, W.-Y. Chen, P.-J. Tsai, K.-Y. Chien, J.-S. Yu, Y.-C. Chen, J. Proteome Res. 6 (2007) 316.
[153] C.-T. Chen, Y.-C. Chen, J. Mass Spectrom. 43 (2008) 538.
[154] J.-C. Liu, P.-J. Tsai, Y.C. Lee, Y.-C. Chen, Anal. Chem. 80 (2008) 5425.
[155] L. Sun, C. Zhang, L. Chen, J. Liu, H. Jin, H. Xu, L. Ding, Anal. Chim. Acta 638 (2009) 162.
[156] C.-T. Chen, Y.-C. Chen, J. Biomed. Nanotechnol. 4 (2008) 73.
[157] M.-A. Coletti-Previero, A. Previero, Anal. Biochem. 180 (1989) 1.
[158] R. Shukla, V. Bansal, M. Chaudhary, A. Basu, R.R. Bhond, M. Sastry, Langmuir 21 (2005) 10644.
[159] Q. Sun, Q. Wang, B.K. Rao, P. Jena, Phys. Rev. Lett. 93 (2004) 186803.
[160] J. Rivas, R.D. Sánchez, A. Fondado, C. Izco, A.J. GarcYa-Bastida, J. García-Otero, J. Mira, D. Baldomir, A. González, I. Lado, M.A. López-Quintela, S.B.

Oseroff, J. Appl. Phys. 76 (1994) 6564.
[161] E.E. Carpenter, C. Sangregorio, C.J. O'Connor, IEEE Trans. Magn. 35 (1999) 3496.
[162] J.-I. Park, J. Cheon, J. Am. Chem. Soc. 123 (2001) 5743.
[163] Z. Ban, Y.A. Barnakov, F. Li, V.O. Golub, C.J. O'Connor, J. Mater. Chem. 15 (2005) 4660.
[164] Y. Shon, G.B. Dawson, M. Porter, R.W. Murray, Langmuir 18 (2002) 3880.
[165] W. Wu, Q. He, H. Chen, J. Tang, L. Nie, Nanotechnology 18 (2007) 145609.
[166] Q. Sun, B.V. Reddy, M. Marquez, P. Jena, C. Gonzalez, Q. Wang, J. Phys. Chem. C 111 (2007) 4159.
[167] Y. Lu, Y. Yin, B.T. Mayers, Y. Xia, Nano Lett. 2 (2002) 183.
[168] Y.H. Deng, C.C. Wang, J.H. Hu, W.L. Yang, S.K. Fu, Colloid Surf. A 26 (2005) 87.
[169] L. Vroman, Science 184 (1974) 585.
[170] X.L. Zhao, Y.L. Shi, Y.Q. Cai, S.F. Mou, Environ. Sci. Technol. 42 (2008) 1201.
[171] X. Zhao, Y. Shi, T. Wang, Y. Cai, G. Jiang, J. Chromatogr. A 1188 (2008) 140.
[172] W. Stöber, A. Fink, E. Bohn, J. Colloid Interface Sci. 26 (1968) 62.
[173] S.-Y. Chang, L. Liu, S.A. Asher, J. Am. Chem. Soc. 116 (1994) 6745.
[174] T. Sen, A. Sebastianelli, I.J. Bruce, J. Am. Chem. Soc. 2006 (128) 7130.
[175] Y. Deng, D. Qi, C. Deng, X. Zhang, D. Zhao, J. Am. Chem. Soc. 130 (2008) 28.
[176] J.H. Scott, S.A. Majetich, Phys. Rev. B 52 (1995) 12564.
[177] M.H. Teng, S.W. Tsai, C.I. Hsiao, Y.D. Chen, J. Alloys Compd. 434-435 (2007) 678.
[178] X. Michalet, F.F. Pinaud, L.A. Bentolila, J.M. Tsay, S. Doose, J.J. Li, Science 307 (2005) 538.
[179] I.L. Medintz, H.T. Uyeda, E.R. Goldman, H. Mattoussi, Nat. Mater. 4 (2005) 435.
[180] J. Gao, H. Gu, B. Xu, Acc. Chem. Res. 42 (2009) 1097.
[181] Y. Wang, J.F. Wong, X. Teng, X.Z. Lin, H. Yang, Nano Lett. 3 (2003) 1555.
[182] S.S. Banerjee, D.-H. Chen, Chem. Mater. 19 (2007) 6345.
[183] L.E. Euliss, S.G. Grancharov, S. O'Brien, Nano Lett. 3 (2003) 1489.
[184] T. Pellegrino, L. Manna, S. Kudera, Nano Lett. 4 (2004) 703.
[185] Y.-M. Huh, Y.-W. Jun, H.-T. Song, J. Am. Chem. Soc. 127 (2005) 12387.
[186] Y.-W. Jun, Y.-M. Huh, J.-S. Choi, J. Am. Chem. Soc. 127 (2005) 5732.
[187] M. Auffan, L. Decome, J. Rose, Environ. Sci. Technol. 40 (2006) 436.
[188] F. Bertorelle, C. Wilhelm, J. Roger, Langmuir 22 (2006) 5385.
[189] M.P. Garcia, R. Miranda Parca, S. Braun Chaves, J. Magn. Magn. Mater. 293 (2005) 277.
[190] Z.P. Chen, Y. Zhang, S. Zhang, J.G. Xia, J.W. Liu, K. Xu, N. Gu, Colloid Surf. A 316 (2008) 210.
[191] C.Ó. Dálaigh, S.A. Corr, Y. Guńko, S.J. Connon, Angew. Chem. 119 (2007) 4407.
[192] A. Hu, G.T. Yee, W. Lin, J. Am. Chem. Soc. 127 (2005) 12486.
[193] J. Hu, G. Chen, I.M.C. Lo, Water Res. 39 (2005) 4528.
[194] H.H. Yang, S.Q. Zhang, X.L. Chen, Z.X. Zhuang, J.G. Xu, X.R. Wang, Anal. Chem. 76 (2004) 1316.
[195] X.L. Pu, Z.C. Jiang, B. Hu, H.B. Wang, J. Anal. Atom. Spectrom. 19 (2004) 984.
[196] C.Z. Huang, B. Hu, J. Sep. Sci. 31 (2008) 760.
[197] B.R. White, B.T. Stackhouse, J.A. Holcombe, J. Hazard. Mater. 161 (2009) 848.
[198] S. Brice-Profeta, M.A. Arrio, E. Tronc, N. Menguy, I. Letard, C. Cartier dit Moulin, M. Nogues, C. Chaneac, J.P. Jolivet, P.H. Saintctavit, J. Magn. Magn. Mater. 288 (2005) 354.
[199] N. De Jaeger, H. Demeye, R. Findy, R. Sneyer, J. Vanderdeelen, P. Van der Meeren, M. Laethem, Part. Part. Syst. Charact. 8 (1991) 179.
[200] H.P. Klug, L.E. Alexander X-ray Diffraction Procedures, New York, Wiley, 1954, p. 512.
[201] K. Inouye, R. Endo, Y. Otsuka, K. Miyashiro, K. Kaneko, T. Ishikawa, J. Phys. Chem. 86 (1982) 1465.
[202] A. Ney, P. Poulopoulos, M. Farle, K. Baberschke, Phys. Rev. B 62 (2000) 11336.
[203] S. Foner, Rev. Sci. Instrum. 30 (1959) 548.
[204] D. Karabelli, C. Üzüm, T. Shahwan, A.E. Eroğlu, T.B. Scott, K.R. Hallam, I. Lieberwirth, Ind. Eng. Chem. Res. 47 (2008) 4758.
[205] S. Gao, Y. Shi, S. Zhang, K. Jiang, S. Yang, Z. Li, E. Takayama-Muromachi, J. Phys. Chem. C 112 (2008)

10398.
[206] D. Zhang, X. Zhang, X. Ni, J. Song, H. Zheng, Cryst. Growth Des. 7 (2007) 2117.
[207] R.N. Grass, E.K. Athanassiou, W.J. Stark, Angew. Chem. Int. Ed. 46 (2007) 4909.
[208] T.M. Vickrey, J.A. Garcia-Ramirez, Sep. Sci. Technol. 15 (1980) 1297.
[209] J. Gorse, T.C. Schunk, M.F. Burke, Sep. Sci. Technol. 19 (1984-85) 1073.
[210] A.H. Latham, R.S. Freitas, P. Schiffer, M.E. Williams, Anal. Chem. 77 (2005) 5055.
[211] J.H. Scott, S.A. Majetich, Phys. Rev. B 52 (1995) 12564.
[212] R.S. Ruoff, D.C. Lorents, B. Chan, R. Malhotra, S. Subramoneg, Science 259 (1993) 346.
[213] M. Todorovic, S. Schultz, J. Wong, A. Scherer, Appl. Phys. Lett. 74 (1999) 2516.
[214] R.D. Shull, IEEE Trans. Magn. 29 (1993) 2614.
[215] H.E. Horng, C.-Y. Hong, S.Y. Yang, H.C. Yang, J. Phys. Chem. Solids 62 (2001) 1749.
[216] R. Zboril, M. Mashlan, D. Petridis, Chem. Mater. 14 (2002) 969.
[217] K.A.J. Gschneidner, V.K. Pecharsky, A.O. Tsokol, Rep. Prog. Phys. 68 (2005) 1479.
[218] S.W. Charles, J. Popplewell, Endeavour. 6 (1982) 153.
[219] R.M. Cornell, U. Schwertmann, The Iron Oxides: Structure, Properties, Reactions, Occurrences and Uses, 2th ed., Wiley-VCH, Weinheim, 2003.
[220] U.T. Lam, R. Mammucari, K. Suzuki, N.R. Foster, Ind. Eng. Chem. Res. 47 (2008) 599.
[221] L. LaConte, N. Nitin, G. Bao, Mater. Today 8 (2005) 32.
[222] A.J. Rosengart, M.D. Kaminski, H. Chen, P.L. Caviness, A.D. Ebner, J.A. Ritter, J. Magn. Magn. Mater. 293 (2005) 633.
[223] G. Iacob, O. Rotariu, N.J. Strachan, U.O. Hafeli, Biorheology 41 (2004) 599.
[224] C.C. Berry, A.S.G. Curtis, J. Phys. D: Appl. Phys. 36 (2003) R198.
[225] H. Gu, K. Xu, C. Xu, B. Xu, Chem. Commun. (2006) 941.
[226] A. Hultgren, M. Tanase, C.S. Chen, G.J. Meyer, D.H. Reich, J. Appl. Phys. 93 (2003) 7554.
[227] J.E. Smith, L. Wang, W. Tan, Trends Anal. Chem. 25 (2006) 848.
[228] C. Xu, K. Xu, H. Gu, X. Zhong, Z. Guo, R. Zheng, X. Zhang, B. Xu, J. Am. Chem. Soc. 126 (2004) 3392.
[229] C. Xu, K. Xu, H. Gu, R. Zheng, H. Liu, X. Zhang, Z. Guo, B. Xu, J. Am. Chem. Soc. 126 (2004) 9938.
[230] H.-H. Hsiao, H.-Y. Hsieh, C.-C. Chou, S.-Y. Lin, A.H.-J. Wang, K.-H. Khoo, J. Proteome. Res. 6 (2007) 1313.
[231] T. Sen, A. Sebastianelli, I.J. Bruce, J. Am. Chem. Soc. 128 (2006) 7130.
[232] K.A. Melzak, C.S. Sherwood, R.F.B. Turner, C.A. Haynes, J. Colloid Interface Sci. 181 (1996) 635.
[233] J.-C. Liu, P.-J. Tsai, Y.C. Lee, Y.-C. Chen, Anal. Chem. 80 (2008) 5425.
[234] A.K. Gupta, M. Gupta, Biomaterials 26 (2005) 3995.
[235] E.H. Kim, H.S. Lee, B.K. Kwak, B.-K. Kim, J. Magn. Magn. Mater. 289 (2005) 328.
[236] J. Wu, Z. Ye, G. Wang, J. Yuan, Talanta 72 (2007) 1693.
[237] R.W. Chantrell, A. Lyberatos, M. El-Hilo, K. O'Grady, J. Appl. Phys. 76 (1994) 6407.
[238] J.L. Dormann, L. Spinu, E. Tronc, J.P. Jolivet, F. Lucari, F. D'Orazio, D. Fiorani, J. Magn. Magn. Mater. 183 (1998) L255.
[239] S. Schneider, S. Rusconi, Biotechniques 21 (1996) 876.
[240] M. Yanase, M. Shinkai, H. Honda, T. Wakabayashi, J. Yoshida, T. Kobayashi, Japan. J. Cancer Res. 89 (1998) 463.
[241] D.C.F. Chan, D.B. Kirpotin, P.A. Bunn, J. Magn. Magn. Mater. 122 (1993) 374.
[242] A. Ito, M. Shinkai, H. Honda, T. Kobayashi, J. Biosci. Bioeng. 100 (2005) 1.
[243] J.A. Gladysz, Chem. Rev. 102 (2002) 3215.
[244] B.M. Bhanage, M. Hrai, Catal. Rev. Sci. Eng. 43 (2001) 315.
[245] A. Nait Ajjou, H. Alper, J. Am. Chem. Soc. 120 (1998) 1466.
[246] N.E. Leadbeater, M. Marco, Chem. Rev. 102 (2002) 3217.
[247] C.A. McNamara, M.J. Dixon, M. Bradley, Chem. Rev. 102 (2002) 3275.
[248] C.E. Song, S.G. Lee, Chem. Rev. 102 (2002) 3495.
[249] P.D. Stevens, J.D. Fan, H.M.R. Gardimalla, M. Yen, Y. Gao, Org. Lett. 7 (2005) 2085.
[250] C. Duanmu, I. Saha, Y. Zheng, B.M. Goodson, Y. Gao, Chem. Mater. 18 (2006) 5973.
[251] R. Abu-Reziq, H. Alper, D.S. Wang, M.L. Post, J. Am.

Chem. Soc. 128 (2006) 5279.
[252] D. Guin, B. Baruwati, S.V. Manorama, Org. Lett. 9 (2007) 1419.
[253] S.J. Ding, Y.C. Xing, M. Radosz, Y.Q. Shen, Macromolecules 39 (2006) 6399.
[254] H.M.R. Gardimalla, D. Mandal, P.D. Stevens, M. Yen, Y. Gao, Chem. Commun. (2005) 4432.
[255] Y. Zheng, C. Duanmu, Y. Gao, Org. Lett. 8 (2006) 3215.
[256] N.T.S. Phan, C.S. Gill, J.V. Nguyen, Z.J. Zhang, C.W. Jones, Angew. Chem. Int. Ed. 45 (2006) 2209.
[257] Y. Sun, X. Li, X.J. Cao, W. Zhang, H.P. Wang, Adv. Colloid Interface Sci. 120 (2006) 47.
[258] P.G. Tratnyek, R.L. Johnson, Nanotoday 1 (2006) 44.
[259] W.-X. Zhang, J. Nanopart Res. 5 (2003) 323.
[260] D.W. Blowes, C.J. Ptacek, S.G. Benner, W.T. McRae Che, T.A. Bennett, R.W. Puls, J. Contam. Hydrol. 45 (2000) 123.
[261] J.T. Nurmi, P.G. Tratnyek, V. Sarathy, D.R. Bear, J.E. Amonette, K. Peacher, C.Wang, J.C. Linehan, D.W. Matson, R.L. Penn, M.D. Driessen, Environ. Sci. Technol. 39 (2005) 1221.
[262] L. Li, M. Fan, R.C. Brown, J.V. Leeuwen, J. Wang, W. Wang, Y. Song, P. Zhang, Crit. Rev. Environ. Sci. Technol. 36 (2006) 405.
[263] Y.-C. Chang, D.-H. Chen, Macromol. Biosci. 5 (2005) 254.
[264] B. Zargar, H. Parham, A. Hatamie, Chemosphere 76 (2009) 554.
[265] S.-Y. Mak, D.-H. Chen, Dyes and Pigments 61 (2004) 93.
[266] A.A. Atia, A.M. Donia, W.A. Al-Amrani, Chem. Eng. J. 150 (2009) 55.
[267] S.-H. Huang, M.-H. Liao, D.-H. Chen, Sep. Purif. Technol. 51 (2006) 113.
[268] P. Li, D.E. Miser, S. Rabiei, R.T. Yadav, M.R. Hajaligol, Appl. Catal. B 43 (2003) 151.
[269] L. Wang, Z. Yang, J. Gao, K. Xu, H. Gu, B. Zhang, X. Zhang, B. Xu, J. Am. Chem. Soc. 128 (2006) 13358.
[270] H.Y. Lee, D.R. Bae, J.C. Park, H. Song, W.S. Han, J.H. Jung, Angew. Chem. Int. Ed. 48 (2009) 1239.
[271] P. Yuan, M. Fan, D. Yang, H. He, D. Liu, A. Yuan, J. Zhu, T. Chen, J. Hazard. Mater. 166 (2009) 821.
[272] J.-F. Liu, Z.-S. Zhao, G.-B. Jiang, Environ. Sci. Technol. 42 (2008) 6949.
[273] S.S. Banerjee, D.-H. Chen, J. Hazard. Mater. 147 (2007) 792.
[274] J. Hu, I.M.C. Lo, G. Chen, Sep. Purif. Technol. 56 (2007) 249.
[275] A.-F. Ngomsik, A. Bee, J.-M. Siaugue, V. Cabuil, G. Cote, Water Res. 40 (2006) 1848.
[276] S.-H. Huang, D.-H. Chen, J. Hazard. Mater. 163 (2009) 174.
[277] W. Yantasee, C.L. Warner, T. Sangvanich, R.S. Addleman, T.G. Carter, R.J. Wiacek, G.E. Fryxell, C. Timchalk, M.G. Warner, Environ. Sci. Technol. 41 (2007) 5114.
[278] P. Wu, Z. Xu, Ind. Eng. Chem. Res. 44 (2005) 816.
[279] S.P. Mulvaney, H.M. Mattoussi, L.J. Whitman, Biotechniques 36 (2004) 602.
[280] N. Gaponik, I.L. Radtchenko, G.B. Sukhorukov, A.L. Rogach, Langmuir 20 (2004) 1449.
[281] D.S. Wang, J.B. He, N. Rosenzweig, Z. Rosenzweig, Nano Lett. 4 (2004) 409.
[282] L. Levy, Y. Sahoo, K.S. Kim, E.J. Bergey, P.N. Prasad, Chem. Mater. 14 (2002) 3715.
[283] V. Salgueirino-Maceira, M.A. Correa-Duarte, M. Spasova, L.M. Liz-Marzan, M. Farle, Adv. Funct. Mater. 16 (2006) 509.
[284] T.R. Sathe, A. Agrawal, S.M. Nie, Anal. Chem. 78 (2006) 5627.
[285] C. Moser, T. Mayr, I. Klimant, Anal. Chim. Acta 558 (2006) 102.
[286] P.S. Eastman, W.M. Ruan, M. Doctolero, R. Nuttall, G. De Feo, J.S. Park, J.S.F. Chu, P. Cooke, J.W. Gray, S. Li, F.Q.F. Chen, Nano Lett. 6 (2006) 1059.
[287] M. Nichkova, D. Dosev, S.J. Gee, B.D. Hammock, I.M. Kennedy, Anal. Biochem. 369 (2007) 34.
[288] A. Loudet, K. Burgess, Chem. Rev. 107 (2007) 4891.
[289] M. Maier, H. Fritz, M. Gerster, J. Schewitz, E. Bayer, Anal. Chem. 70 (1998) 2197.
[290] K. Turney, T.J. Drake, J.E. Smith, W. Tan, W.W. Harrison, Rapid Commun. Mass Spectrom. 18 (2004) 2367.
[291] H.H. Yang, S.Q. Zhang, X.L. Chen, Z.X. Zhuang, J.G. Xu, X.R. Wang, Anal. Chem. 76 (2004) 1316.
[292] C.T. Chen, Y.C. Chen, Anal. Chem. 77 (2005) 5912.
[293] S.V. Kolotilov, P.N. Boltovets, B.A. Snopok, V.V. Pavlishchuk, Theor. Exp. Chem. 42 (2006) 211.
[294] P.R. Sudhir, H.F. Wu, Z.C. Zhou, Anal. Chem. 77

(2005) 7380.
[295] J.K. Herr, J.E. Smith, C.D. Medley, D.H. Shangguan, W.H. Tan, Anal. Chem. 78 (2006) 2918.
[296] B.N.Y. Vanderpuije, G. Han, V.M. Rotello, R.W. Vachet, Anal. Chem. 78 (2006) 5491.
[297] Z.M. Saiyed, M. Parasramka, S.D. Telang, C.N. Ramchand, Anal. Biochem. 363 (2007) 288.
[298] X.X. He, H.L. Huo, K.M. Wang, W.H. Tan, P. Gong, J. Ge, Talanta 73 (2007) 764.
[299] P.C. Lin, M.C. Tseng, A.K. Su, Y.J. Chen, C.C. Lin, Anal. Chem. 79 (2007) 3401.
[300] S.Y. Chang, N.Y. Zheng, C.S. Chen, C.D. Chen, Y.Y. Chen, C.R.C. Wang, J. Am. Soc. Mass Spectrom. 18 (2007) 910.
[301] K. Moeller, J. Kobler, T. Bein, Adv. Funct. Mater. 17 (2007) 605.
[302] K.J. Klabunde, Nanoscale Material in Chemistry, Wiley-Interscience, New York, 2001.
[303] Y.S. Lin, P.J. Tsai, M.F. Weng, Y.C. Chen, Anal. Chem. 77 (2005) 1753.
[304] J.E. Smith, C.D. Medley, Z. Tang, D. Shangguan, C. Lofton, W. Tan, Anal. Chem. 79 (2007) 3075.
[305] P.J. Robinson, P. Dunnill, M.D. Lilly, Biotechnol. Bioeng. 15 (1973) 603.
[306] J.D. Li, Y.Q. Cai, Y.L. Shi, S.F. Mou, G.B. Jiang, J. Chromatogr. A 1139 (2007) 178.
[307] F.J. López-Jiménez, S. Rubio, D. Pérez-Bendito, Anal. Chim. Acta 551 (2005) 142.
[308] J. Li, X. Zhao, Y. Shi, Y. Cai, S. Mou, G. Jiang, J. Chromatogr. A 1180 (2008) 24.
[309] L. Sun, C. Zhang, L. Chen, J. Liu, H. Jin, H. Xu, L. Ding, Anal. Chim. Acta 638 (2009) 162.
[310] H. Parham, N. Rahbar, J. Pharm. Biomed. Anal. 50 (2009) 58.
[311] Y.R. Song, S.L. Zhao, P. Tchounwou, Y.M. Liu, J. Chromatogr. A 1166 (2007) 79.
[312] M. Faraji, Y. Yamini, A. Saleh, M. Rezaee, M. Ghambarian, R. Hassani, Anal. Chim. Acta 659 (2010) 172.
[313] B. Zargar, H. Parham, A. Hatamie, Talanta 77 (2009) 1328.
[314] M. Faraji, Y. Yamini, M. Rezaee, Talanta (in press, doi:10.1016/j.talanta.2010.01.023).
[315] H. Parham, N. Rahbar, Talanta 80 (2009) 664.
[316] Y. Sha, C. Deng, B. Liu, J. Chromatogr. A 1198-1199 (2008) 27.
[317] Y. Liu, H. Li, J.-M. Lin, Talanta 77 (2009) 1037.
[318] C. Huang, B. Hu, J. Sep. Sci. 31 (2008) 760.
[319] C. Huang, B. Hu, Spectrochim. Acta Part B 63 (2008) 437.
[320] J.S. Suleiman, B. Hu, H. Peng, C. Huang, Talanta 77 (2009) 1579.
[321] G. Wulff, Angew. Chem. Int. Ed. 34 (1995) 1812.
[322] B. Sellergren, Molecularly Imprinted Polymers Man-made Mimics of Antibodies and their Application in Analytical Chemistry, Elsevier, New York, 2001.
[323] C.H. Lu, W.H. Zhou, B. Han, H.H. Yang, X. Chen, X.R. Wang, Anal. Chem. 79 (2007) 5457.
[324] D. Gao, Z. Zhang, M. Wu, C. Xie, G. Guan, D. Wang, J. Am. Chem. Soc. 129 (2007) 7859.
[325] C. Ki, J. Chang, Macromolecules 39 (2006) 3415.
[326] H. Yang, S. Zhang, F. Tang, Z. Zhuang, X. Wang, J. Am. Chem. Soc. 127 (2005) 1378.
[327] C. Xie, B. Liu, Z.Wang, D. Gao, G. Guan, Z. Zhang, Anal. Chem. 80 (2008) 437.
[328] H. Wang,W. Zhou, X. Yin, Z. Zhuang, H. Yang, X.R. Wang, J. Am. Chem. Soc. 128 (2006) 15954.
[329] R.J. Ansell, K. Mosbach, Analyst 123 (1998) 1611.
[330] Y. Li, X.F. Yin, F.R. Chen, H.H. Yang, Z.X. Zhang, X.R. Wang, Macromolecules 39 (2006) 4497.
[331] C.J. Tan, H.G. Chua, K.H. Ker, Y.W. Tong, Anal. Chem. 80 (2008) 683.
[332] X. Wang, L. Wang, X. He, Y. Zhang, L. Chen, Talanta 78 (2009) 327.
[333] N. Kirsch, M.J. Whitcombe, in: M. Yan, O. Ramström (Eds.), Molecularly Imprinted Materials Science and Technology, Marcel Dekker, 2005, Chap. 5.
[334] Z. Lu, Y. Qin, J. Fang, J. Sun, J. Li, F. Liu, W. Yang, Nanotechnology 19 (2008) 055602.
[335] S.J. Son, J. Reichel, B. He, M. Schuchman, S.B. Lee, J. Am. Chem. Soc. 127 (2005) 7316.
[336] Y. Deng,C. Deng, D. Yang, C. Wang, S. Fu, X. Zhang, Chem. Commun. (2005) 5548.
[337] L. Limback, R. Bereiter, E. Müller, R. Krebs, R. Gälli, W.J. Stark, Environ. Sci. Technol. 42 (2008) 5828.